DEPARTMENT OF THE NAVY

HYDROMECHANICS

O

AERODYNAMICS

O

STRUCTURAL MECHANICS

O

APPLIED MATHEMATICS

O

ACOUSTICS AND VIBRATION

EXPERIMENTAL MEASUREMENTS OF THE STEADY LIFT, DRAG, AND MOMENT ON SURFACE-PIERCING STRUTS

by

Gene M. Wilburn
and H. Smith Haller, Jr.

HYDROMECHANICS LABORATORY
RESEARCH AND DEVELOPMENT REPORT

October 1965 Report 1778

EXPERIMENTAL MEASUREMENTS OF THE STEADY LIFT, DRAG, AND MOMENT ON SURFACE-PIERCING STRUTS

by

Gene M. Wilburn
and H. Smith Haller, Jr.

October 1965

Report 1778

TABLE OF CONTENTS

LIST OF FIGURES

NOTATION

AR	Aspect ratio $= S/c^2$
c	Chord length of the foil (ft.)
C_D	Drag coefficient = $D/ \frac{1}{2} \rho V^2 S$
C_L	Lift coefficient = $L/ \frac{1}{2} \rho V^2 S$
C_M	Moment coefficient = $M/ \frac{1}{2} \rho V^2 Sc$
D	Drag (lb)
F_c	Froude number based on chord length $FC = V \sqrt{cg}$
g	Acceleration of gravity (ft. /sec.^{2})
L	Lift (lb.)
M	Moment (lb/ ft)
R_e	Reynolds number based on chord length = Vc/ν
S	Submerged area of foil (ft. ^{2})
V	Velocity of foil (ft. /sec.)
α	Angle between model chord and the direction of the free-stream velocity (degrees)
ρ	Density of the water 1.936 (slugs/ft. ^{3})
ν	Kinematic coefficient of viscosity of water 1.055×10^{-5} (ft. ^{2}/sec.)

ABSTRACT

Testing of two surface-piercing strut configurations for the TMB Pitch-Heave Oscillator is described. Experimental measurements were made of the steady lift, drag, and moment on two rectangular planform, finite aspect ratio struts at finite Froude numbers. The first model section had identical symmetrical ogival fairings on the leading and trailing edges and a flat center section. For the second configuration the aft ogive fairing was cut off the first model section, and a square trailing edge was left. The model force and moment coefficients are presented and the wake, spray, and cavitation characteristics of both profiles are discussed.

Preliminary computations of the theoretical pressure distributions for 8 two-dimensional sections and computed full-scale forces and moments for the PHO-2 strut configuration are included.

ADMINISTRATIVE INFORMATION

This work is authorized under the Hydrofoil Accelerated Research Program, Bureau of Ships letters SF011-0201 Serial 420-255 of 3 October 1962 and Serial 341 B-125 of 13 August 1963. The work was supported under SS 600 000, Task 1703.

INTRODUCTION

The design of a pitch-heave oscillator (PHO-2) to test two-dimensional hydrofoil models was undertaken at the David Taylor Model Basin for the Bureau of Ships Hydrofoil Accelerated Research Program. This oscillator (Figure 1) will be mounted on Carriage 5 in the TMB high-speed towing tank and will drive the test foil sinusoidally in either heave or pitch. Tests will be conducted with various test foil submergences and surface conditions at carriage speeds up to 45 knots. The horizontal test foil (6-foot span, 24-inch maximum chord) will be supported between two, vertical surface-piercing struts, which will house the oscillator mechanisms and act as end plates. This report describes a preliminary test which was designed to establish the section geometry of these struts according to the following criteria:

1. The flow is to be smooth and unaccelerated between the struts where the model foil will be mounted.
2. There is to be no cavitation near the test foil.
3. The strut is to provide sufficient volume for the strut structure and pitch-heave oscillator mechanism.
4. Minimum hydrodynamic forces and moments are to be exerted on the strut.
5. The strut is to have a low weight.

Measured forces and moments are presented in coefficient form for two strut sections. Appendix B contains dimensional forces and moments which have direct application to the PHO-2.

GENERAL DESIGN CONSIDERATIONS

The strut will be a straight untapered surface with a constant section. To provide unaccelerated flow and to allow for motion of the foil relative to the strut, the strut surface must be flat for at least 48 inches in the fore-and-aft direction in the region where the foil attaches to the oscillator mechanism. Preliminary calculations showed that a maximum thickness of 7 inches for this part of the strut would satisfy the volume requirement. For minimum forces and moment the strut first must have a symmetrical section. Second it must have the minimum chord dimension that is consistent with the first three criteria. This minimum chord length also satisfies the low-weight requirement.

Since no published data could be found which was directly applicable to this problem, Mr. John L. Power conducted a computer study of the theoretical two-dimensional pressure distributions for eight symmetrical faired flat sections; see Figure A2 in Appendix A. Two sections were selected for testing; see Figure 2. The first profile, Section A, was chosen on the basis of having a short chord, smoothly varying pressure gradient, and a minimum pressure coefficient sufficient to prevent cavitation at the maximum test speed. Basically, Section A is a flat panel

with identical ogival leading and trailing edge fairings; this profile will be called the double-faired strut. To investigate the flow conditions for a strut of minimum area, the trailing edge fairing was cut off Section A, leaving a square trailing edge. This second profile, Section B, will be called the modified strut.

The full-scale strut is designed to run with the bottom tip submerged at various depths between 36 and 72 inches below the water surface. The test hydrofoil is mounted 24 inches above the tip of this strut.

TEST

TEST PROCEDURE

One-sixth-scale models of the double-faired surface-piercing strut and the modified surface-piercing strut were tested on Carriage 3 in the high-speed towing tank. The Section A model was machined from aluminum and was hand-finished to the desired profile; see Figure 2. The leading edge was made particularly sharp to reveal any tendency of the model to cavitate. To obtain the Section B profile, the aft ogive fairing was cut off the original model. Forces and moments were measured with the TMB three-component dynamometer. Three aspects of this test were significant in designing the full-scale strut: (1) the values of lift, drag, and moment coefficients for various chord Froude numbers and submergence aspect ratios, (2) the cavitation tendencies of the models, and (3) the spray and wake characteristics of each strut. Runs were made to simulate Froude numbers through and beyond the full-scale speed range.

The Froude number based on chord length c is $F_c = V/\sqrt{cg}$ where V is velocity and g is the gravitational constant. Carriage speeds from 5 to 30 knots simulated full-scale speeds from 12.25 to 73.50 knots. Froude numbers ranged from 1.377 to 8.259 for the double-faired strut and from 3.108 to 9.323 for the modified strut. Submergences of both model strut tips were 6, 8, 10, and 12 inches. The corresponding submergence aspect ratios for Section A, with a 14-inch chord, were 0.429, 0.571, 0.715, and 0.858. Submergence aspect ratios for Section B, with an 11-inch chord, were 0.545, 0.728, 0.910, and 1.090. The model submergences corresponded to full-scale submergences of 3, 4, 5, and 6 feet respectively. Angle of attack was varied up to a maximum of 18 degrees at a speed of 5 knots. For speeds between 10 and 25 knots, the maximum angle of attack was generally 5 degrees. At speeds above 25 knots and at deeper submergences the load range of the dynamometer generally limited to angle of attack to less than 5 degrees.

APPARATUS

The three components of the hydrodynamic force in the horizontal plane are measured with the DTMB Three Component Dynamometer. The force-sensing elements are six hydraulic load cells. Each load cell is connected to a readout gage on the dynamometer. The cells are mounted in pairs in the same horizontal plane and are arranged so that only one in each pair is loaded at any one time. In this system it is possible to zero each cell individually to eliminate zero drift. The first pair of load cells measures drag or

or thrust. The second pair measures side force (lift) at a point 1 foot forward of the dynamometer axis. The third pair also measures the side force component but at a point 1 foot aft of the dynamometer axis. This system is insensitive to forces in the vertical direction.

All load cells were claibrated from zero to 100 pounds with dead weights applied with cables and pulleys to a loading bar installed in place of the model; see Figure 3. The loads could be applied individually or simultaneously to any combination of the six loading points. Each point was chosen to load a particular cell; see Figure 3. The cells were loaded individually to check for independence. No cross coupling was found. The reading accuracy was plus or minus one-quarter of a pound for lift and plus or minus one-eighth of a pound for drag. Repeatability was well within the reading accuracy of the gages.

The model was cantilever supported from the bottom of a dynamometer shaft which was specially modified for this test (TMB Drawing No. E-1841-1). The original shaft was shortened and a clamp was provided for the model so that its fore-and-aft position relative to the dynamometer axis could be adjusted. This adjustment allowed the load distribution between the front and back load cells to be changed for best utilization of the dynamometer capacity. The angle of attack (angle between the model chord plane and the direction of carriage travel) was set by rotating the dynamometer shaft with a worm wheel. The smallest division on the angle of attack vernier was 0. 1 degree. The foil submergence was set by

raising or lowering the dynamometer and attached foil relative to the carriage and then clamping the dynamometer in place.

This dynamometer has several characteristics which limit its usefulness for a test program of this type. First, the maximum permissible loads restricted the speeds for the deeper submergences at high angles of attack. Next, the number of speed conditions which could be tested in one carriage run was limited because considerable time was necessary for the read-out gages to stabilize, particularly the drag component gage. This was caused by the lag in the hydraulic load cell system and the inertia of the model and balance assembly. Third, the spanwise location of the center of pressure could not be determined because the dynamometer is insensitive to moments about any horizontal axis.

Force readings on the dynamometer gages were photographed as well as recorded manually to eliminate the possibility of recording errors in the short test time during multiple speed runs. During typical runs 16-mm motion pictures were taken of the model wake and spray to supplement visual observations of the test. These films are on file in the TMB film library under No. M 0045.

TEST DATA

The recorded force data were corrected using the dynamometer correction curves in Figure 4. From these corrected values the model lift, drag, and moment referred to the center of the flat foil section were obtained. The lift, drag, and moment coefficients were computed based

on the submerged area of each model.

The lift coefficients of Sections A and B versus angle of attack are shown in Figures 5 and 6. In particular, it was noted that even though the area of the modified model (Section B) was less than the area of the double-faired model (Section A), the total lift force was greater. Figure 5A shows the variation in C_L due to Froude number for Section A at a low aspect ratio (AR = 0.429) as well as the decrease in the lift slope with increasing angle of attack. Froude number effect almost disappears for aspect ratios above 0.571 for the double-faired section and above 0.728 for the modified section. Observe that with increasing aspect ratios the slope of the lift coefficient curve increases for both Section A and Section B. Further it is noteworthy that at an aspect ratio as low as 0.728 for the modified strut and 0.715 for the double-faired strut, the classical relationship of C_L as a linear function of α is closely approximated although the value of the lift curve slope for infinite aspect ratio has not been reached. The effect of cavitation on the lift coefficient of Section B is evident from Figure 6. At cavitation inception, the lift decreases abruptly but the lift curve slope beyond this point remains unchanged.

The drag coefficient curves versus angle of attack are shown in Figures 7 and 8. Figures 9 and 10 show C_D versus Froude number at an angle of attack of 0.5 degree for the two configurations. The drag coefficient for the double-faired strut is a more complicated function of Froude number and submergence than for the modified strut. However,

at the maximum test submergence, at low angles of attack, and at high speed, the total drag is approximately the same for the two profiles.

The moment coefficients versus angle of attack are shown in Figures 11 and 12. Froude number and aspect ratio variations have less effect on the moment coefficient than on the lift coefficient. Similarly, the change in moment coefficient for Section B due to cavitation is much less than the corresponding change in lift coefficient under the same conditions.

WAKE AND CAVITATION

The double-faired model had a smoother wake than the modified shape and had no cavitation except at high angles of attack (complete separation occurred on the low-pressure side at about a 10-degree angle of attack during the 5-knot runs). At low angles of attack the leading edge wave wetted both strut surfaces and rose sharply to a considerable height (possibly as high as one chord length at high speed). The flow around the modified model was similar to that of the double-faired shape as far back as the trailing edge. However, at this discontinuity a stable fully ventilated cavity formed, and at high speed there was a rooster tail and more spray than with the double-faired shape.

As speed and angle of attack of the modified shape were increased at shallow submergences, cavitation occurred at a point on the bottom tip, on the low pressure side, where the ogive radius is tangent to the flat section. Upon inception the cavity immediately propagated to the

ventilated cavity at the trailing edge. This condition was normally accompanied by a small area of cavitation along the leading edge at the tip of the strut. This cavitation extended further upward towards the surface as speed or angle of attack increased. The various stages of cavitation encountered by Section B are illustrated in Figure 13. From the motion pictures taken of the pressure side of the model, the leading edge cavitation is seen and the side cavity is partially visible at the tip.

DISCUSSION

It is not possible to take all conditions into account in a limited test such as this. Hence, the exact effect of geometrical scale on spray and wake characteristics was not determined. Further, it was considered impractical to simulate some conditions found on the actual PHO-2, i. e., the loads and asymmetry of flow due to the junction of the test foil with the strut and the effect of the mutual interference of the two struts. The primary concern was proper Froude number scaling to obtain the force and moment coefficients.

The full-scale-strut coefficients were extrapolated from the model data by using the following assumptions:

1. Cavitation causes no coefficient changes with variation of geometrical scale.
2. The lift coefficient is not dependent on Reynolds number in the range encountered in this test (R_e = 7.3 x 10^5 to 5.58 x 10^6).

3. The moment coefficient is dependent only on the lift coefficient.
4. The induced drag coefficient is dependent only on the lift coefficient.
5. The frictional drag coefficient is dependent only on the Reynolds number.
6. Wave and form drag coefficients are dependent only on the Froude number.

From assumptions 1 and 2 the lift and moment coefficients are assumed to be the same as for the full-scale strut at the same Froude number. Since the lift coefficient and Froude number stay the same, there will be no change in the induced, form, and wave drag coefficients. However, the frictional drag coefficient was corrected for Reynolds number by the Schoenherr method.[1]

Some of the assumptions used to compute the full-scale data (Appendix B) might be questionable if it were not that the main area of interest is at low angles of attack where no cavitation or other extreme condition is expected. For example, the effect on C_L of increasing R_e is only apparent in the region of maximum C_L, which is beyond the operating angle of attack for the PHO-2 struts.

---

1 References are listed on page 45.

For the full-scale strut it is assumed that the maximum angle of attack due to mechanical misalignment, angularity of flow, and distortion under load will be less than one-fourth of a degree. At this angle of attack the double-faired strut (Shape A) generates slightly less lift than the mofified strut (Shape B). However, the total lift for a single strut will be less than 2000 pounds at 50 knots for either profile. Shape B has a much smaller hydrodynamic moment than A. Any deflection due to moment will increase the angle of attack and, thus, will increase the loads even further. It is, therefore, important to have as low a moment as possible. The difference between the drag for the two strut configurations is small for low angles of attack. The modified shape has the lower drag. In any event, the drag of either shape will be less than 3000 pounds (per strut) at 50 knots. Based on model tests at angles of attack less than 2 degrees, it is expected that at all speeds and submergences the full-scale double-faired strut will not cavitate whereas the full-scale modified strut will have only the nonobjectionable ventilated cavity at the trailing edge. Based on these results, profile B was selected for the PHO-2 strut section. In Appendix B, full-scale forces and moment for profile B are presented for small angles of attack and various submergences.

CONCLUSIONS

Both strut sections would give negligible interference to the flow over the test foil. The bow wave and spray of both profiles would be severe enough that some form of spray shield would be necessary. The

ventilated cavity at the trailing edge of strut B would not interfere with the flow over the test hydrofoil. Strut A would not cavitate. Nevertheless, Section B was selected because of the following advantages:

1. Lower hydrodynamic twisting moment.
2. Lower weight and smaller chord.
3. Simpler construction.
4. Slightly lower drag.

ACKNOWLEDGMENTS

The authors wish to thank Mr. John L. Power for his preparation of the computer study of various strut profiles and his assistance in conducting the test program. We are also grateful to Messrs. John Pattison and William Souders for assistance in data reduction and preparation of the curves.

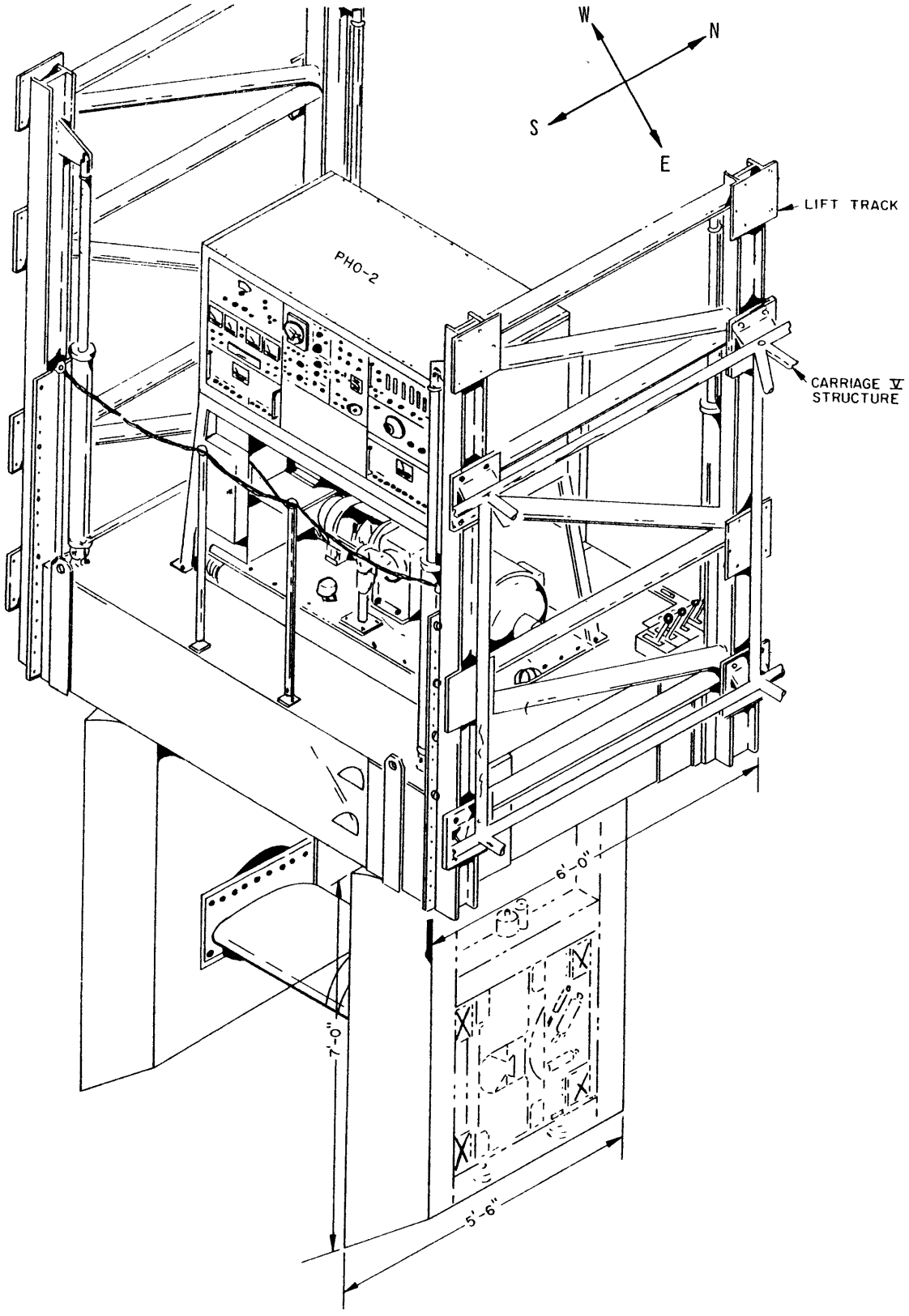

FIGURE 1 - PITCH-HEAVE OSCILLATOR

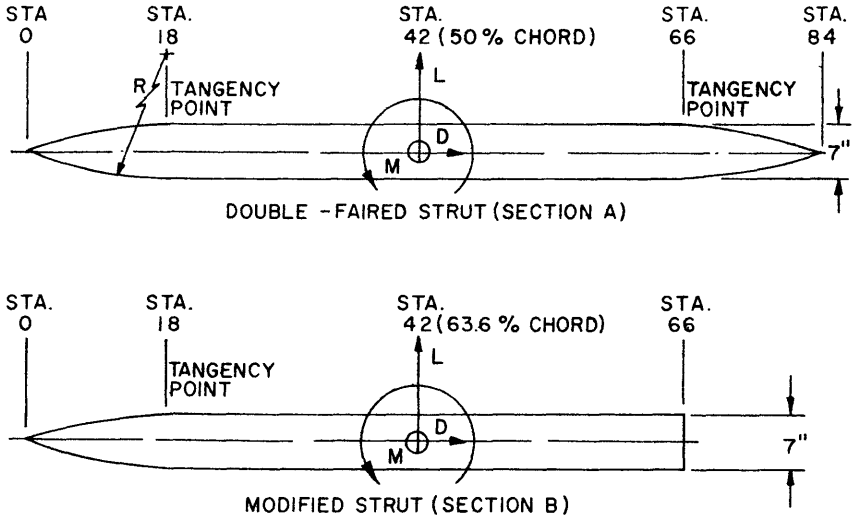

FIGURE 2 - STRUT SECTIONS

Stations are inches from the leading edge for the full-scale strut.

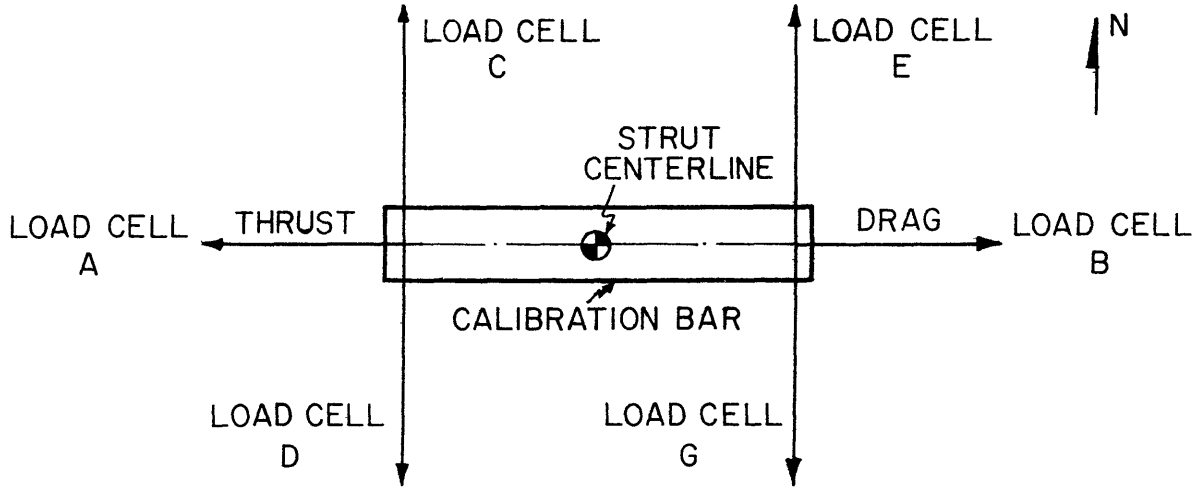

Dynamometer Load Cell Arrangement (Top View)

FIGURE 3 - CALIBRATION BAR

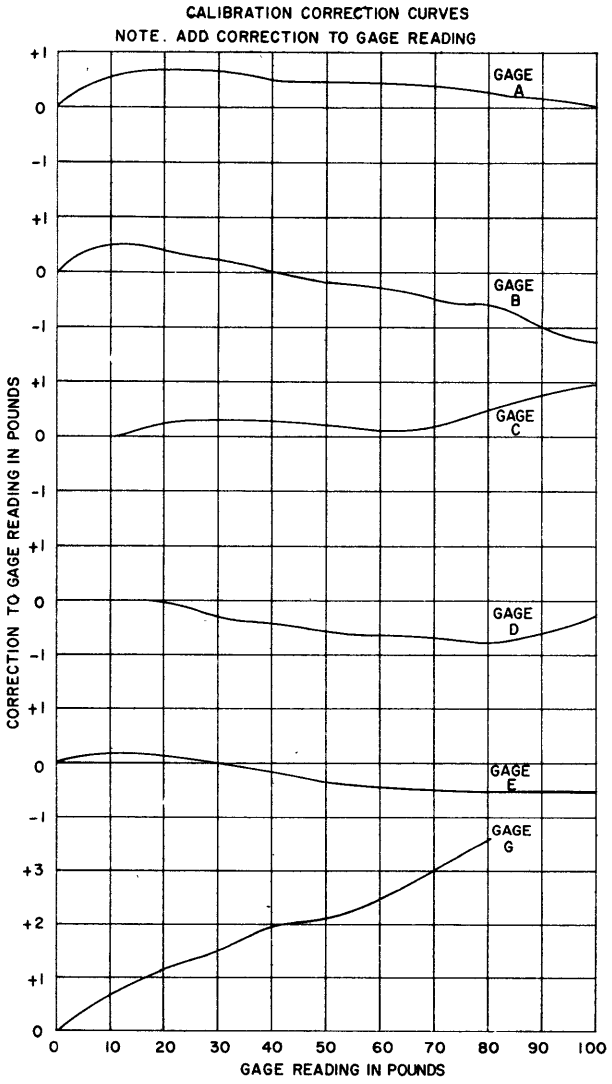

FIGURE 4 - CALIBRATION CORRECTION CURVES

FIGURE 5 - LIFT COEFFICIENT VERSUS ANGLE OF ATTACK FOR SECTION A

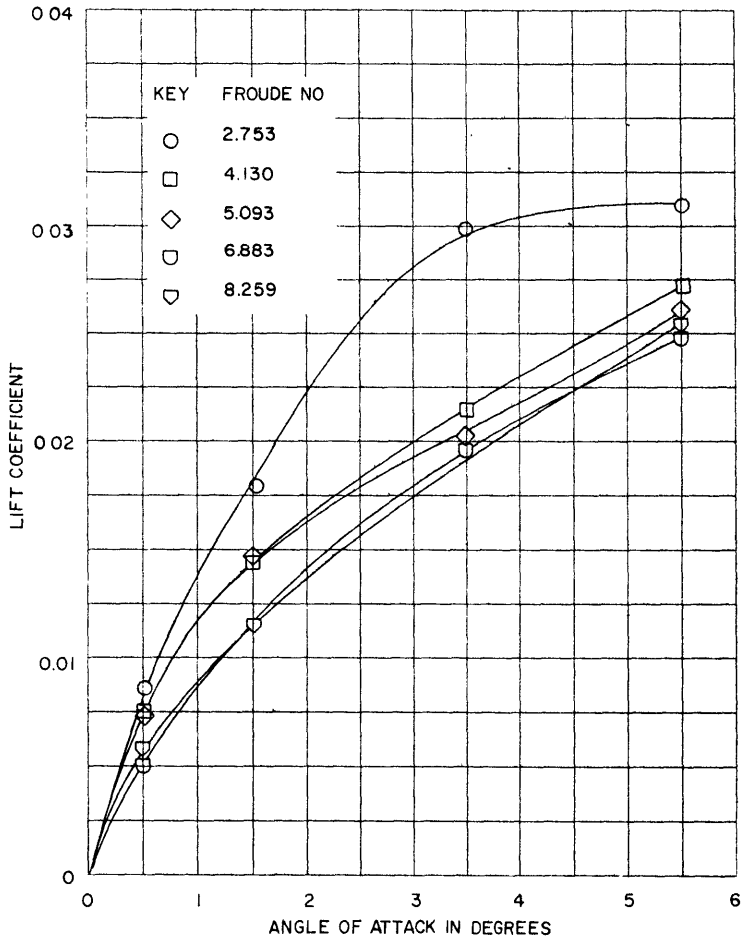

Figure 5a – Aspect Ratio = 0.429, Froude Number 2.753 to 8.259

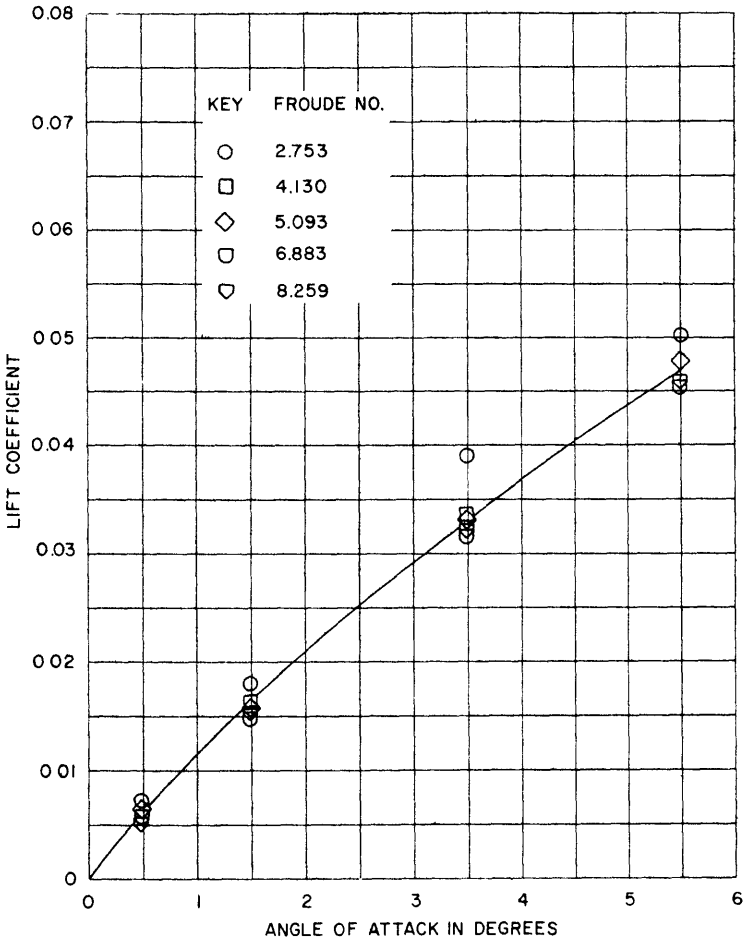

Figure 5b – Aspect Ratio = 0.571, Froude Number 2.753 to 8.259

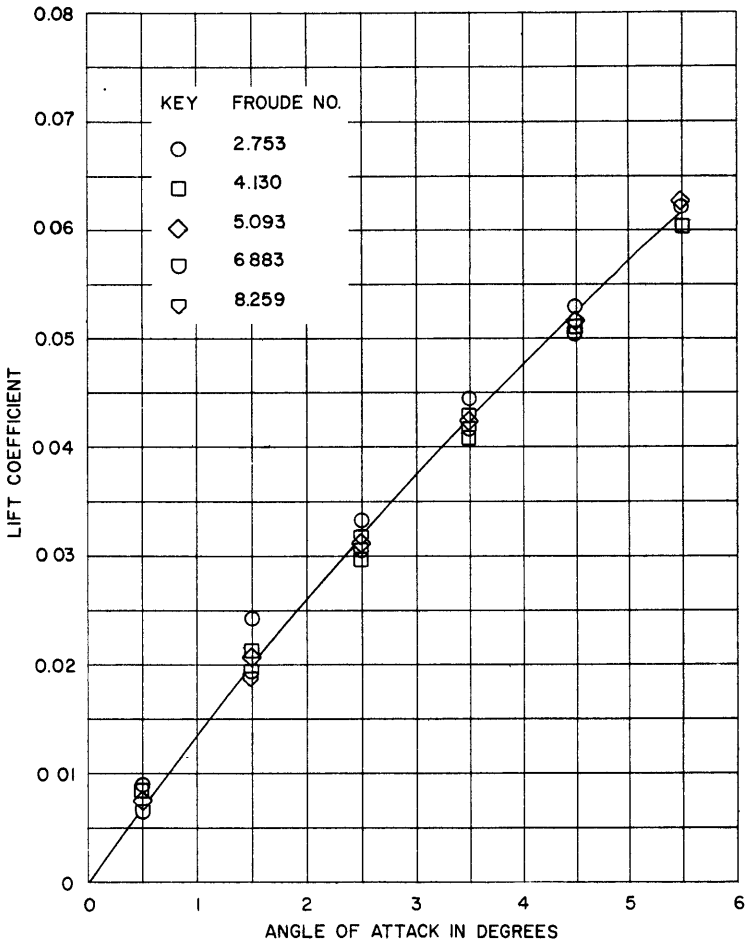

Figure 5c — Aspect Ratio = 0.715, Froude Number 2.753 to 8.259

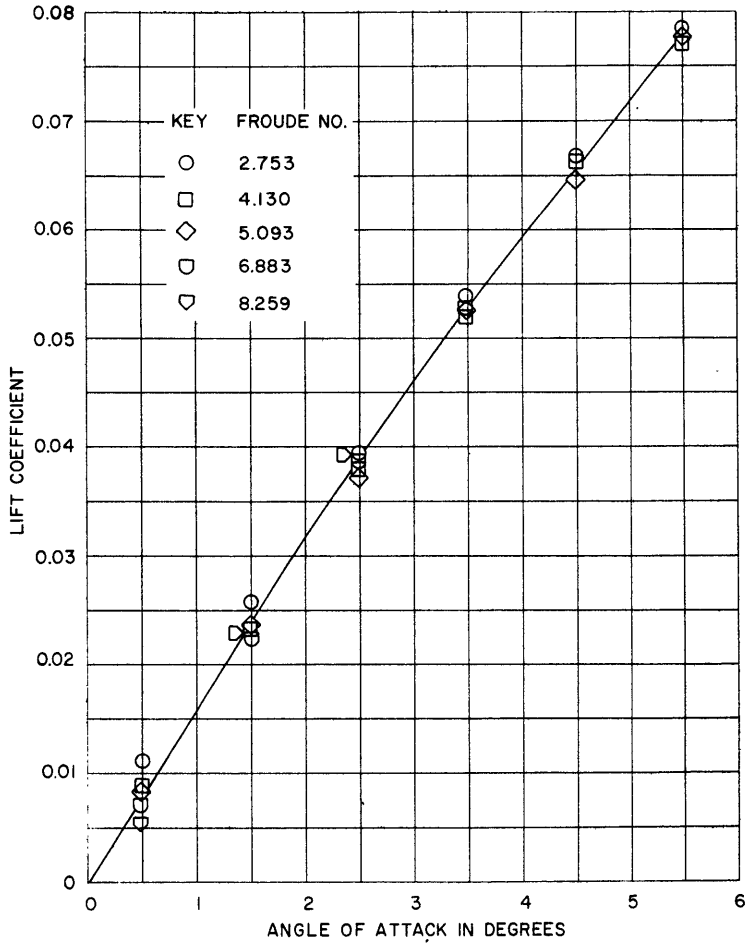

Figure 5d — Aspect Ratio = 0.858, Froude Number 2.753 to 8.259

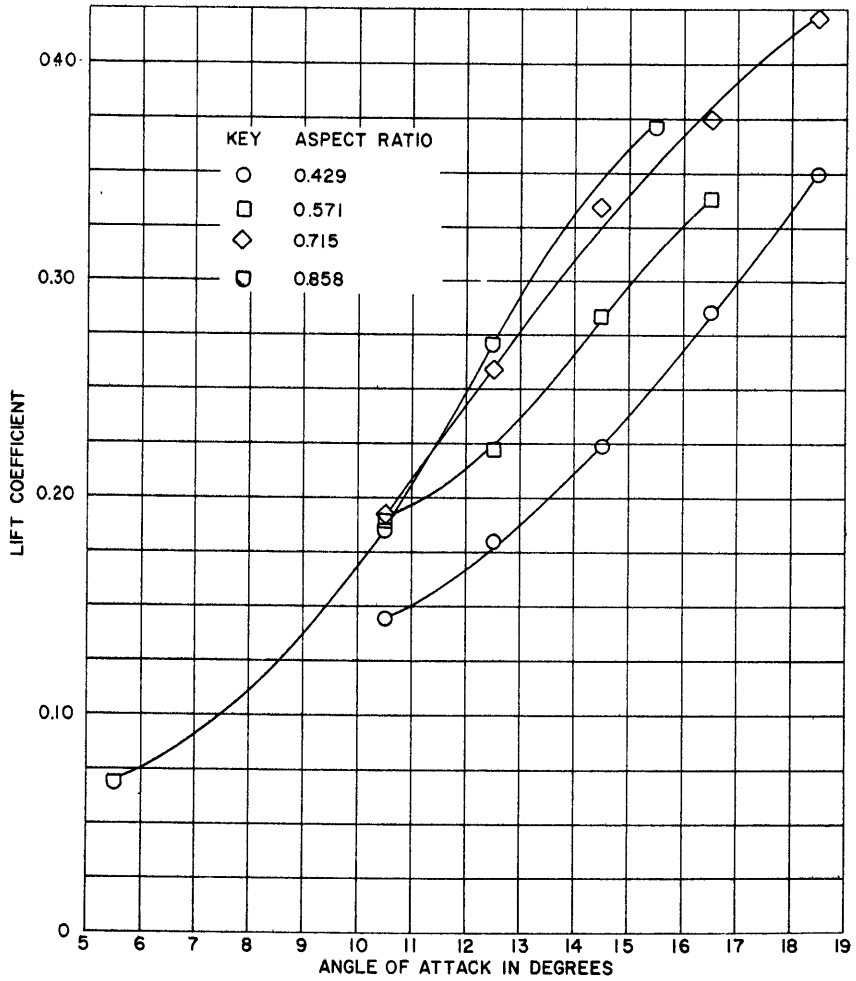

Figure 5e – Froude Number = 1.377, Aspect Ratios 0.429 to 0.858

FIGURE 6 - LIFT COEFFICIENT VERSUS ANGLE OF ATTACK FOR SECTION B

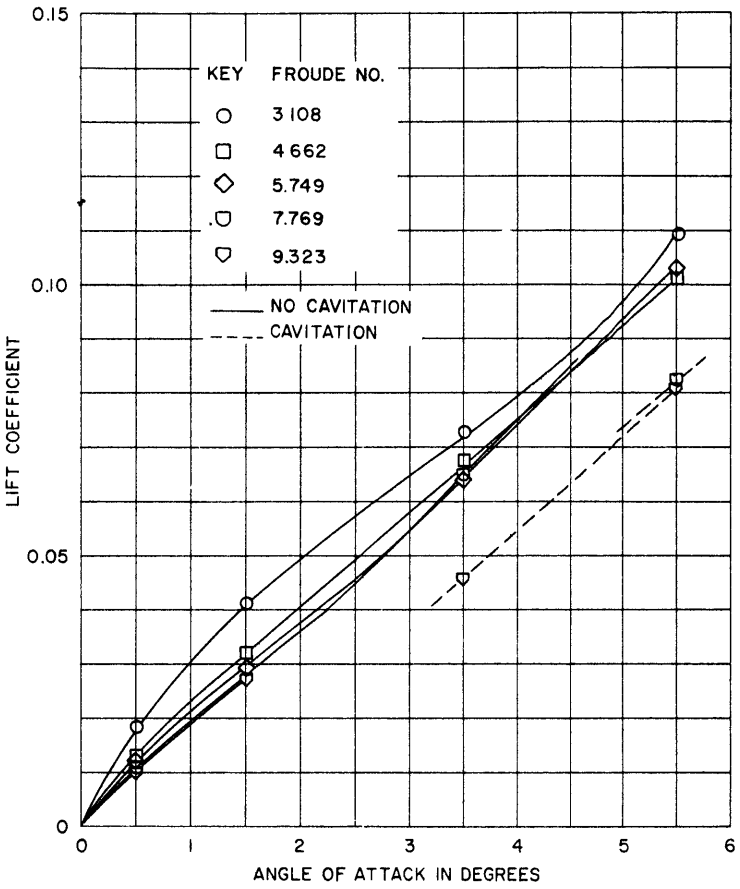

Figure 6a – Aspect Ratio = 0.545, Froude Number 3.108 to 9.323

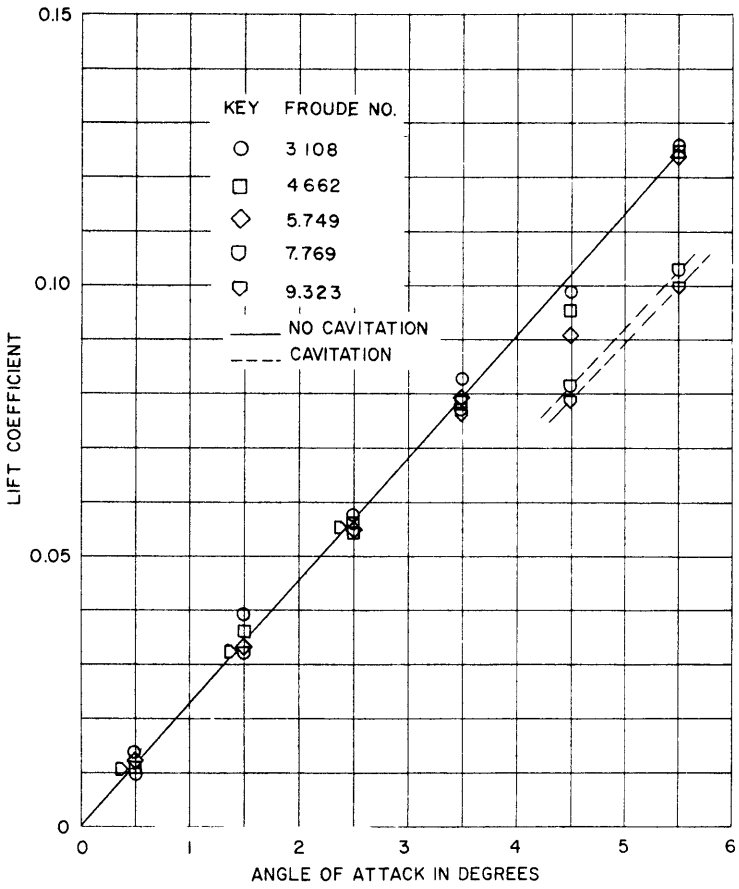

Figure 6b – Aspect Ratio = 0.728, Froude Number 3.108 to 9.323

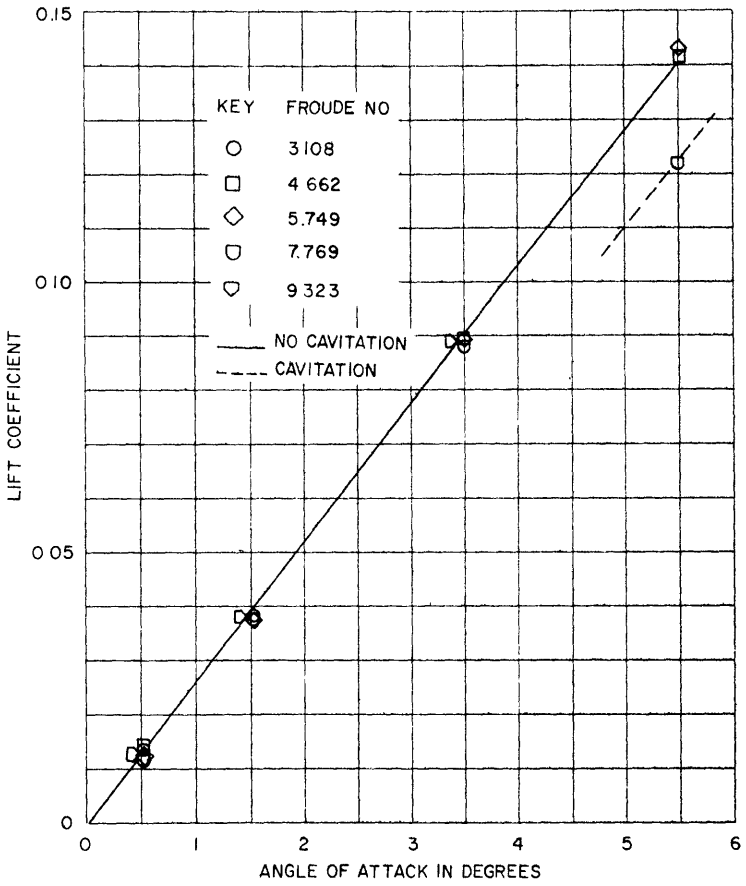

Figure 6c – Aspect Ratio = 0.910, Froude Number 3.108 to 9.323

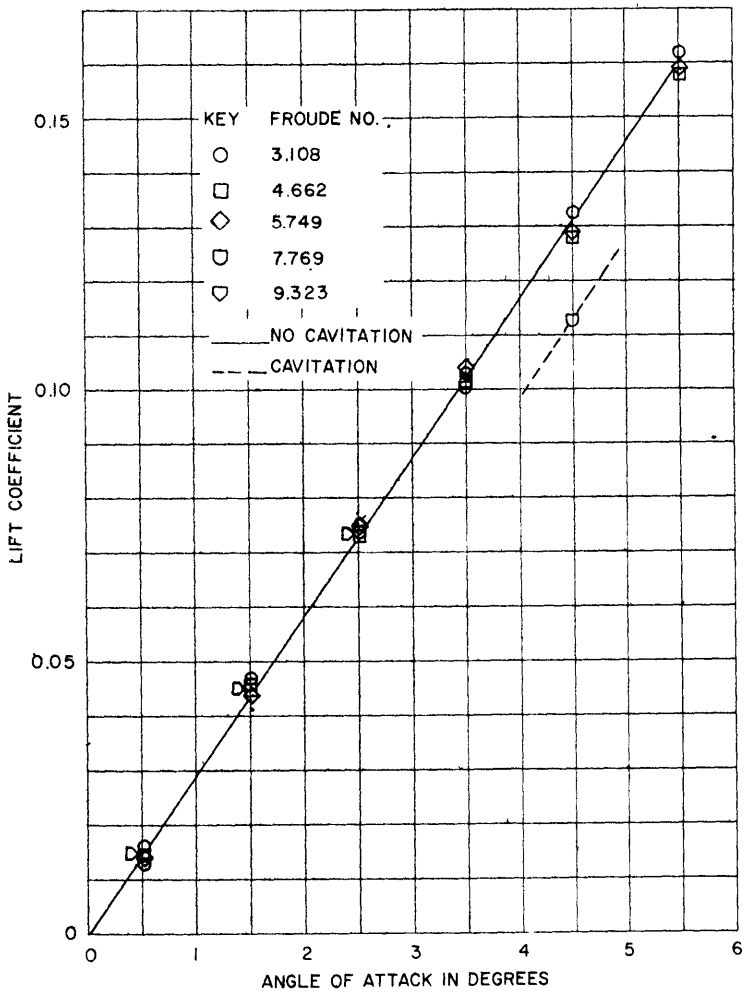

Figure 6d – Aspect Ratio = 1.090, Froude Number 3.108 to 9.323

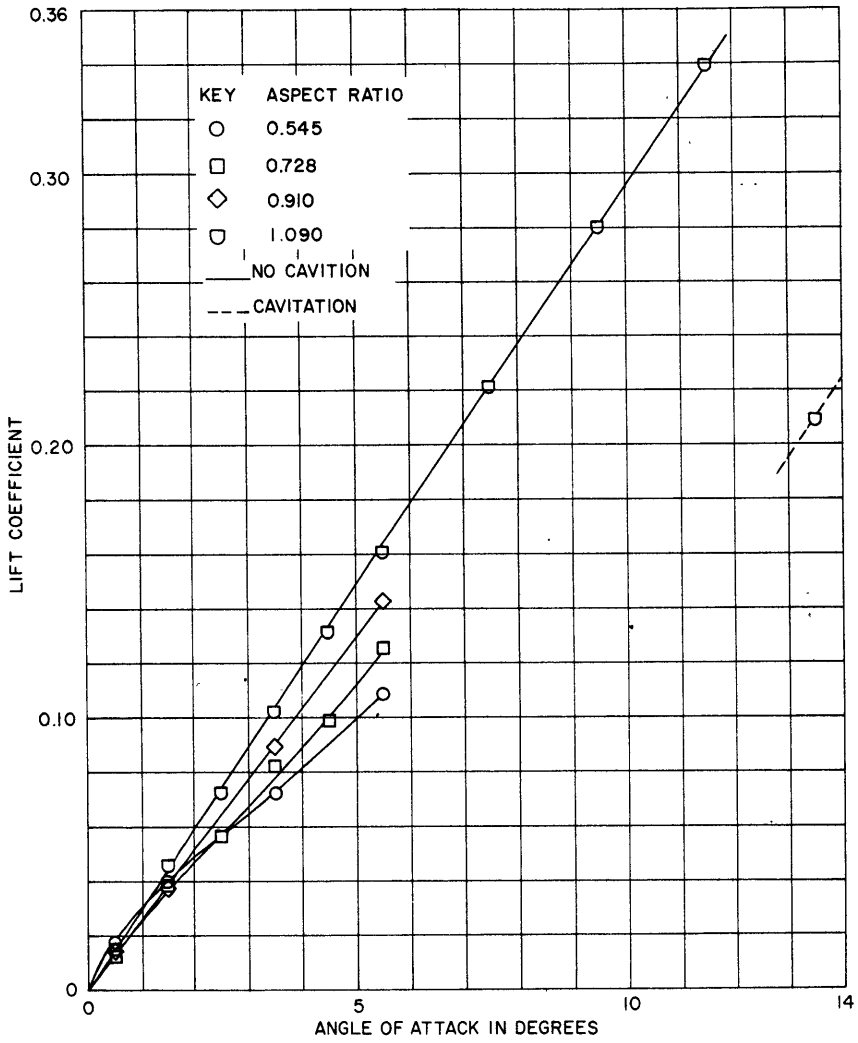

Figure 6e – Froude Number = 3.108, Aspect Ratios 0.545 to 1.090

FIGURE 7 - DRAG COEFFICIENT VERSUS ANGLE OF ATTACK FOR SECTION A

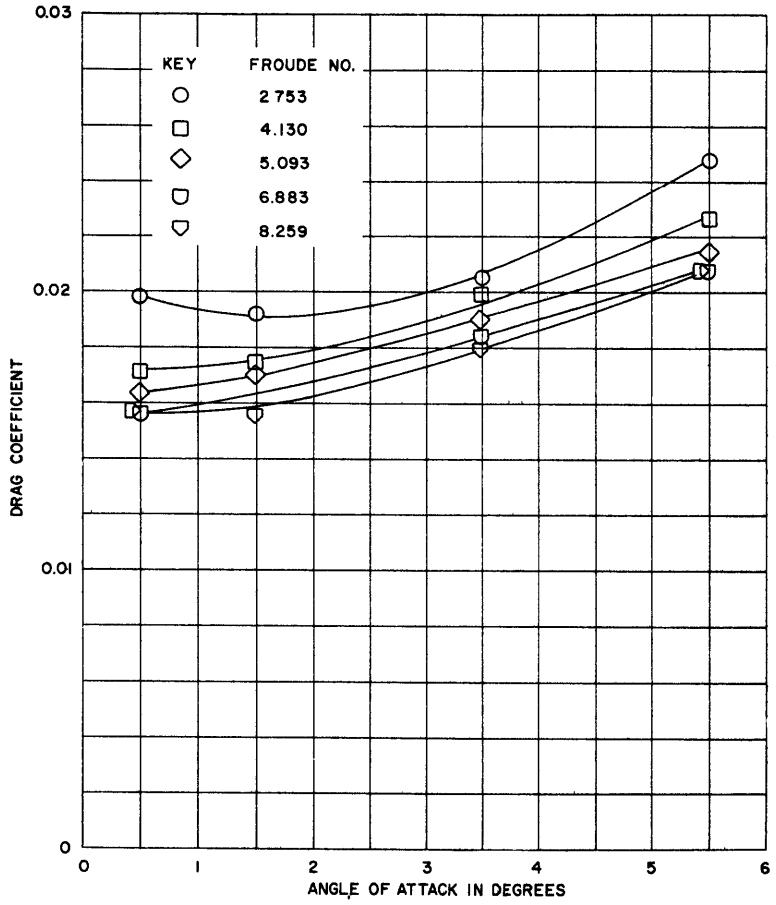

Figure 7a – Aspect Ratio = 0.429, Froude Number 2.753 to 8.259

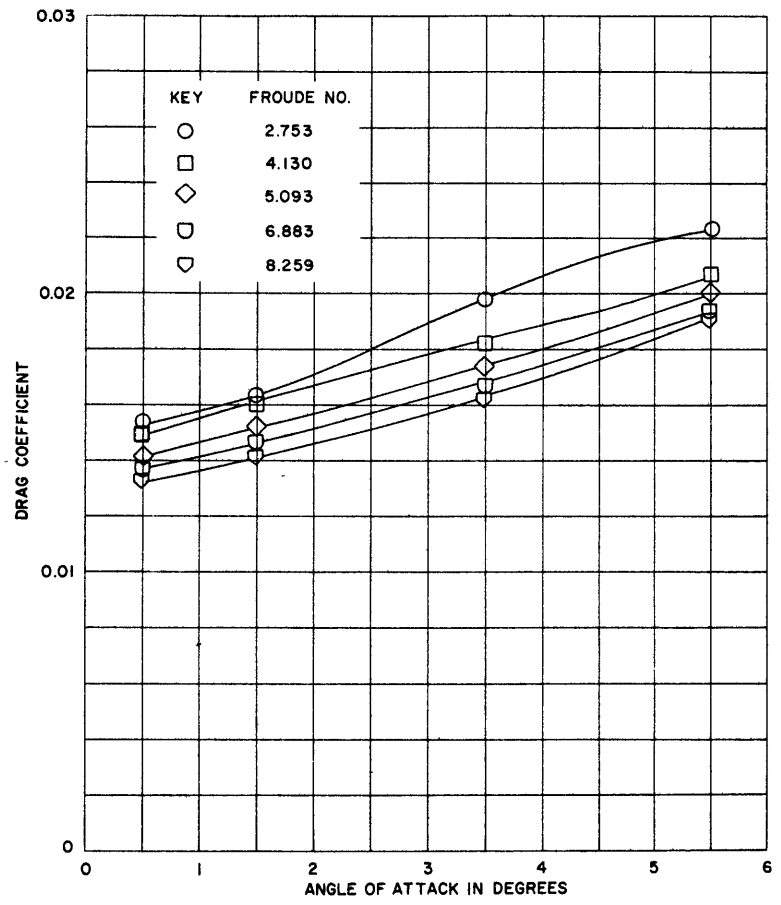

Figure 7b – Aspect Ratio = 0.571, Froude Number 2.753 to 8.259

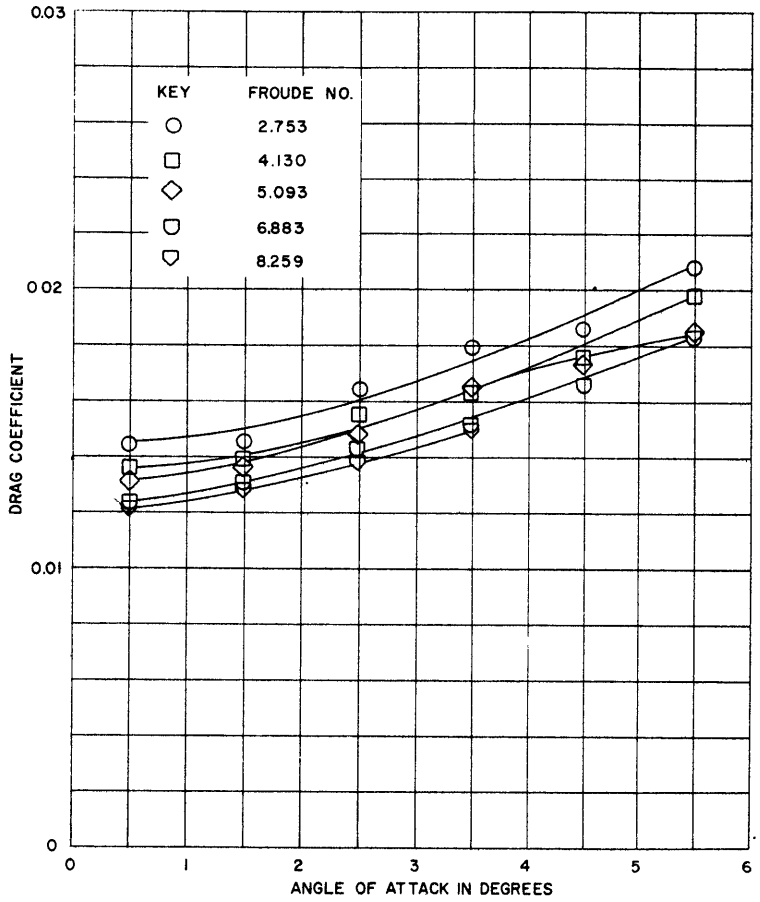

Figure 7c – Aspect Ratio = 0.715, Froude Number 2.753 to 8.259

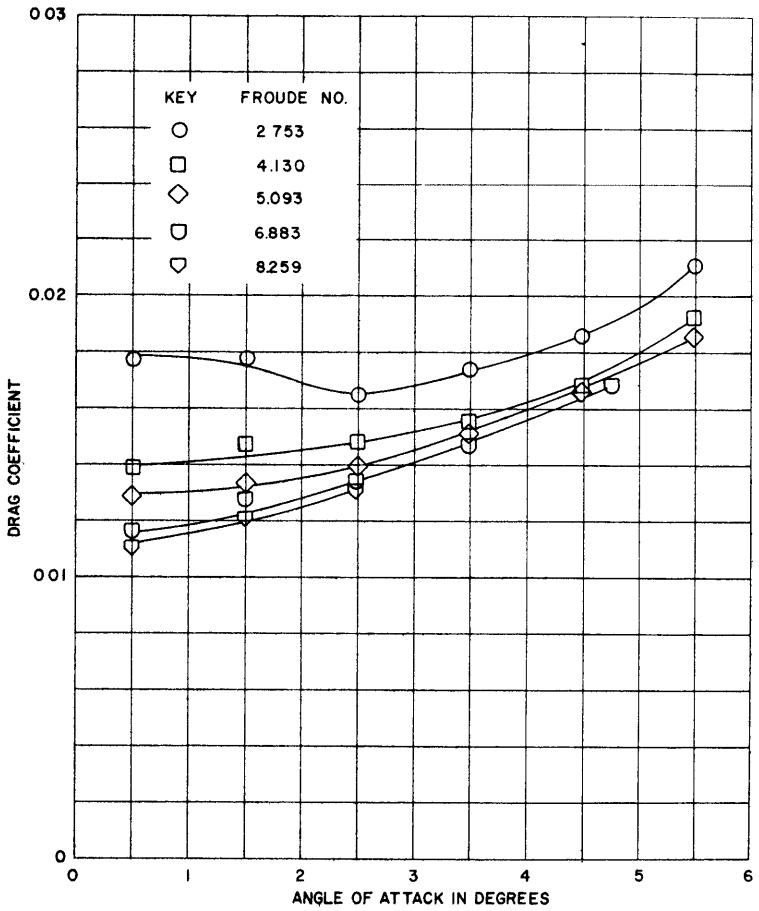

Figure 7d – Aspect Ratio = 0.858, Froude Number 2.753 to 8.259

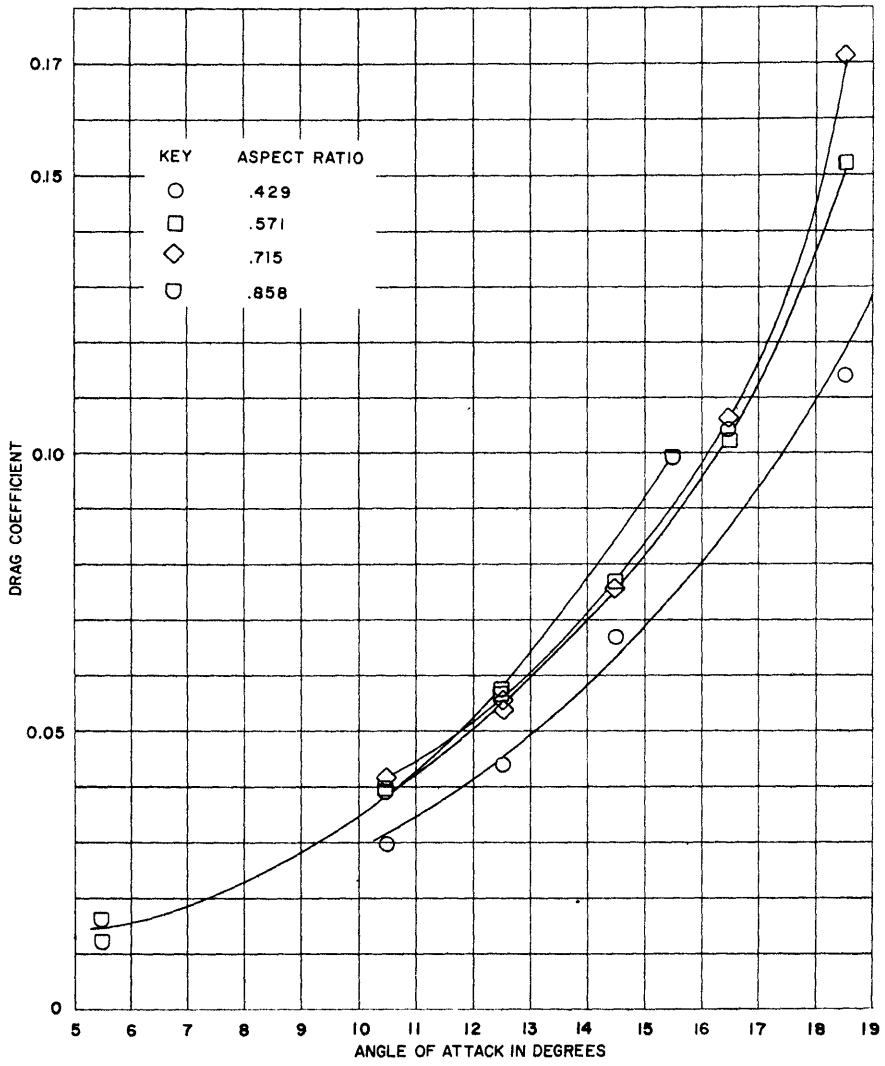

Figure 7e – Froude Number = 1.377, Aspect Ratios 0.429 to 0.858

FIGURE 8 - DRAG COEFFICIENT VERSUS ANGLE OF ATTACK FOR SECTION B

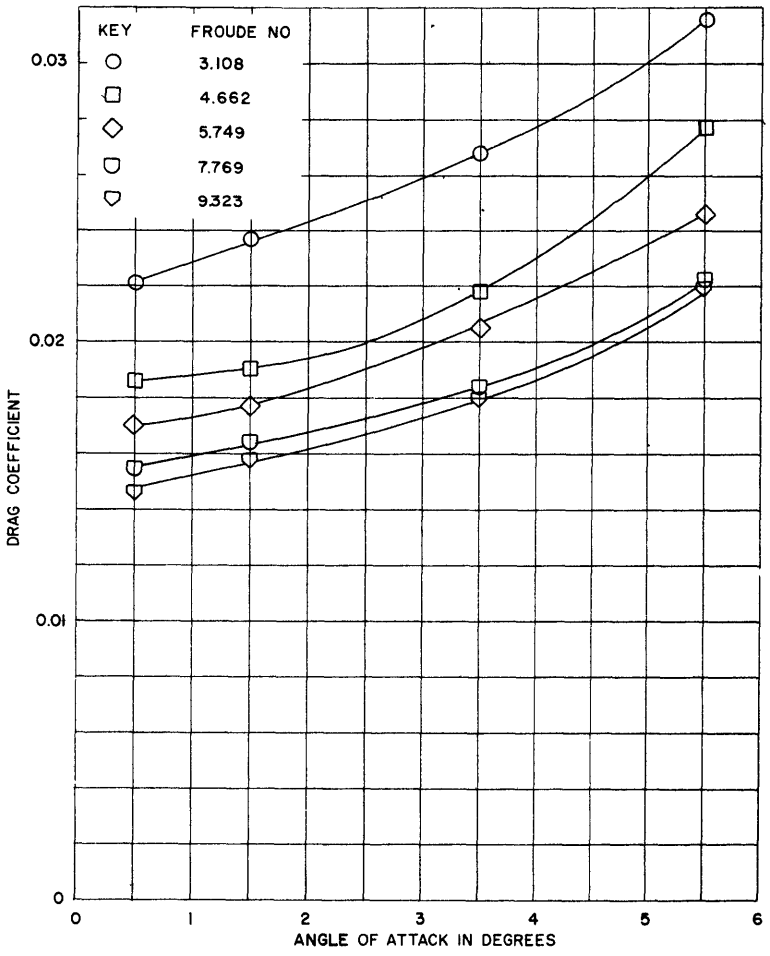

Figure 8a – Aspect Ratio = 0.545, Froude Number 3.108 to 9.323

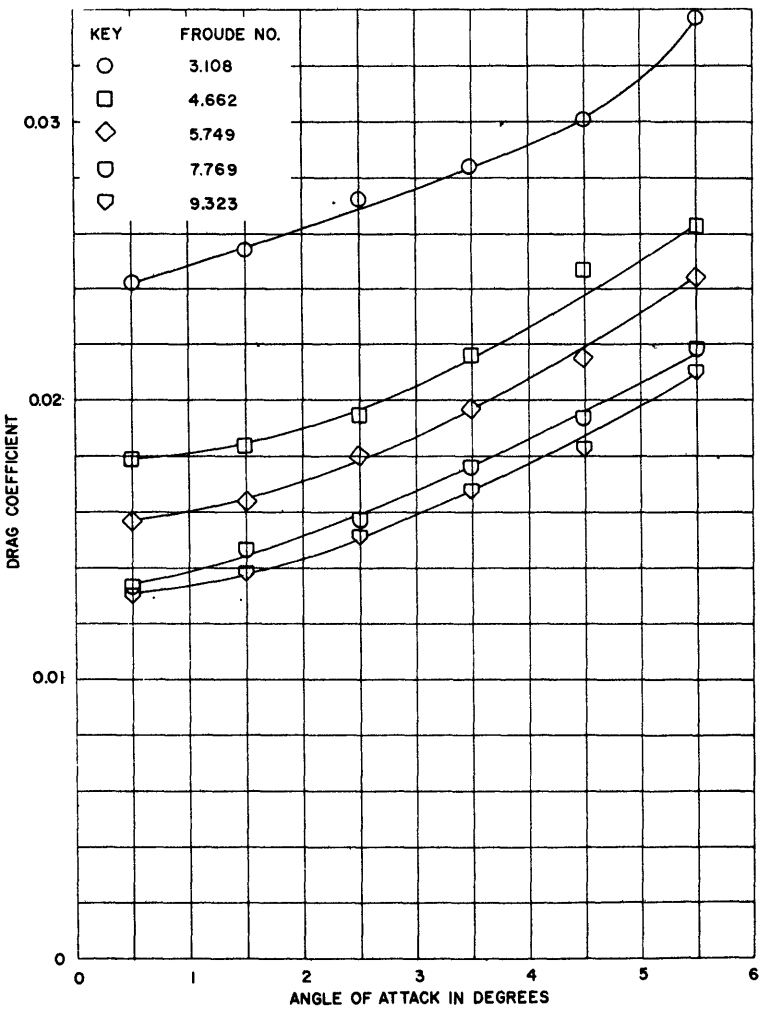

Figure 8b – Aspect Ratio = 0.728, Froude Number 3.108 to 9.323

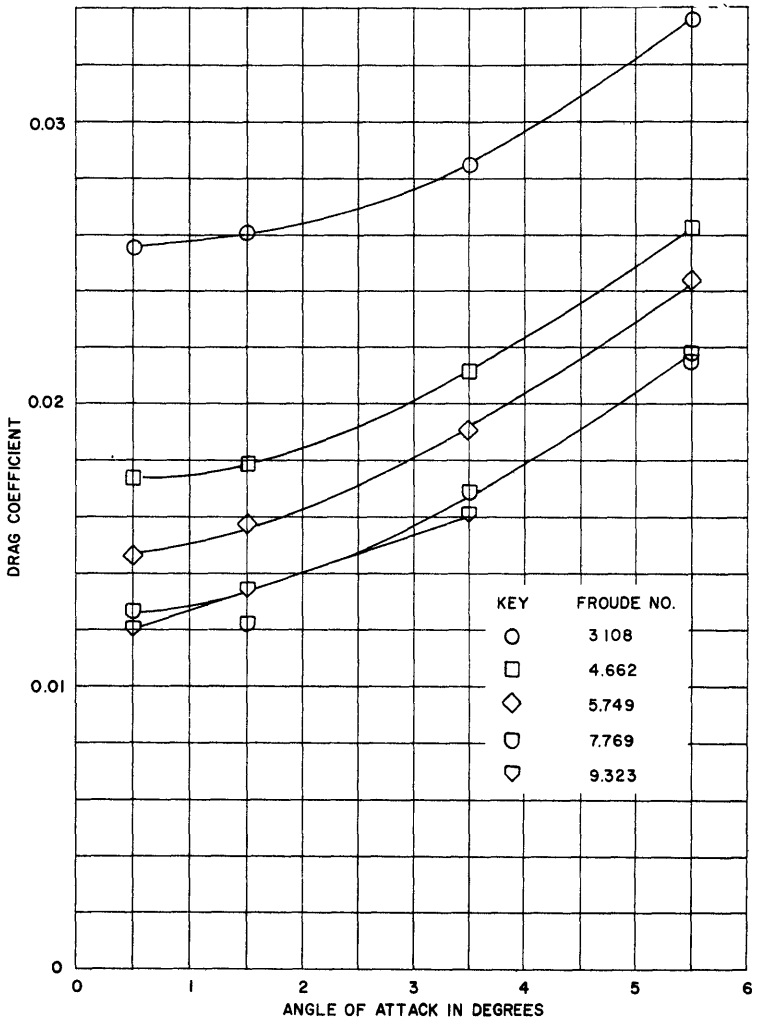

Figure 8c – Aspect Ratio = 0.910, Froude Number 3.108 to 9.323

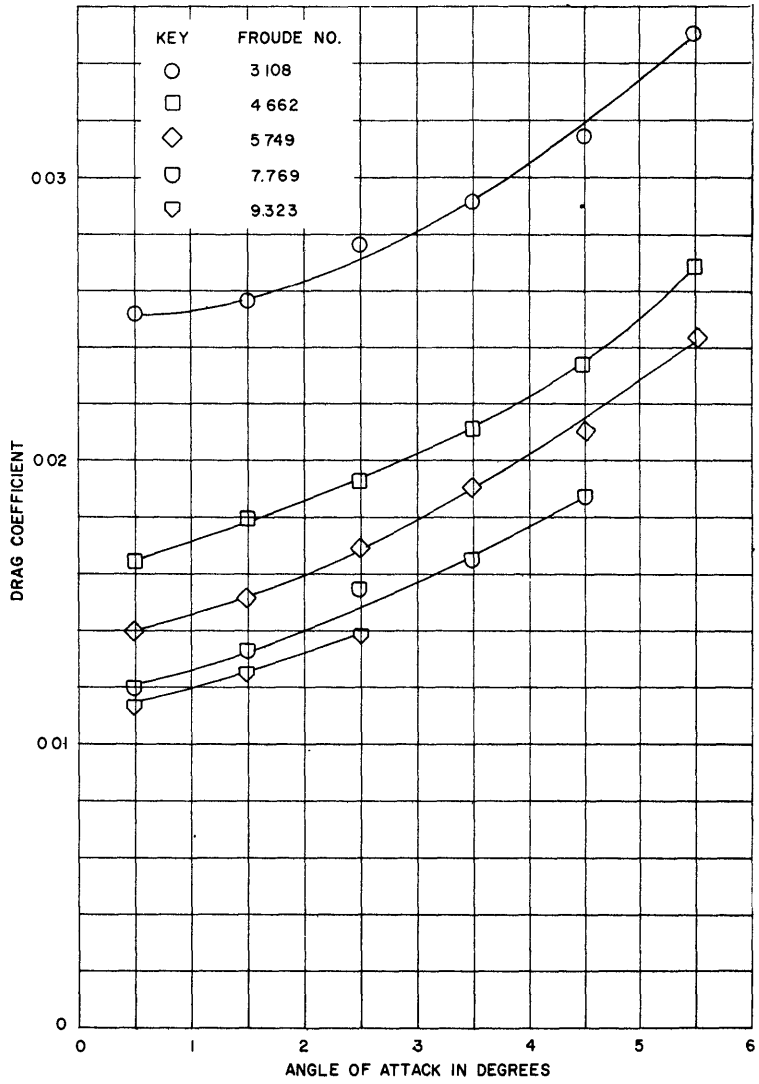

Figure 8d – Aspect Ratio = 1.090, Froude Number 3.108 to 9.323

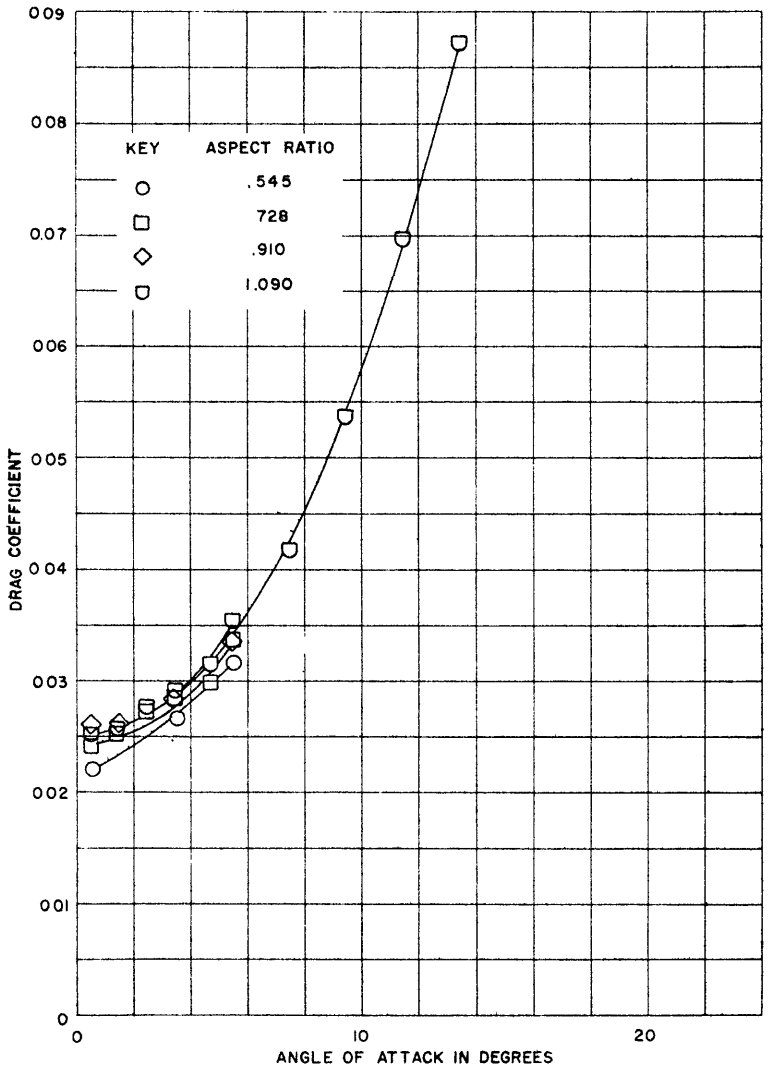

Figure 8e – Froude Number = 3.108, Aspect Ratios 0.545 to 1.090

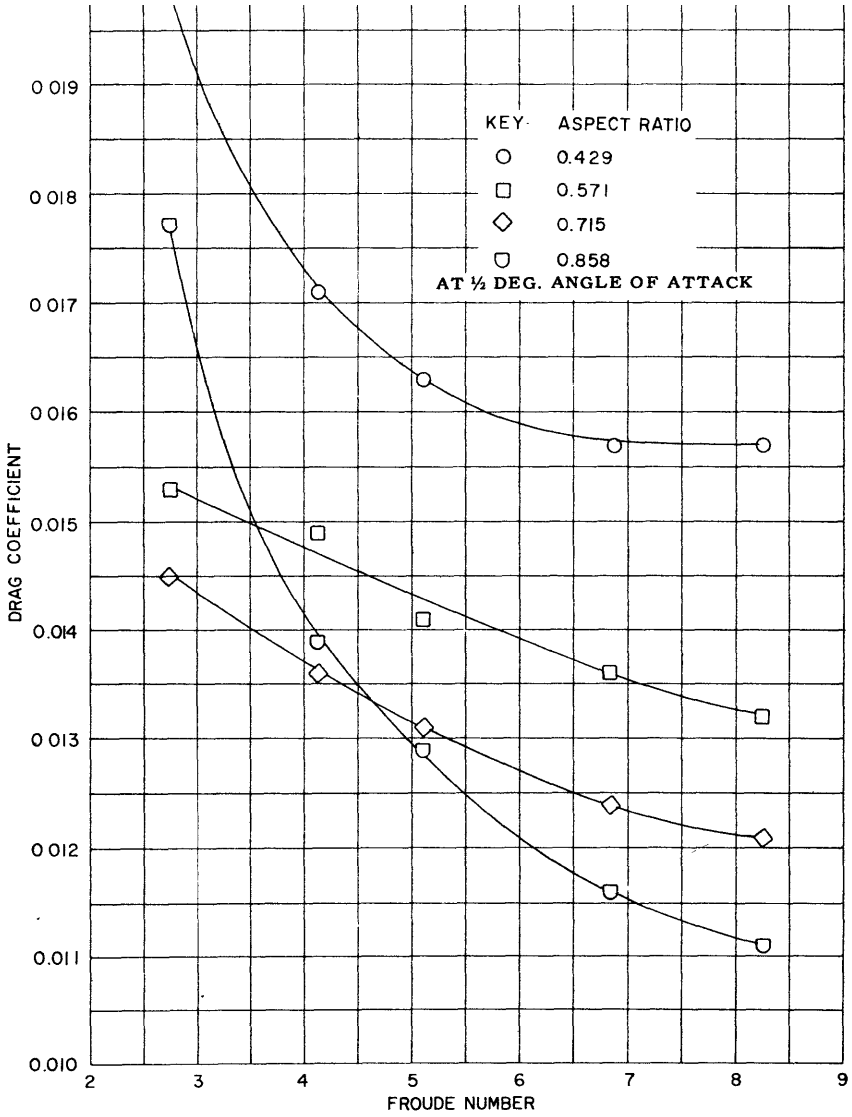

FIGURE 9 - DRAG COEFFICIENT VERSUS FROUDE NUMBER FOR SECTION A

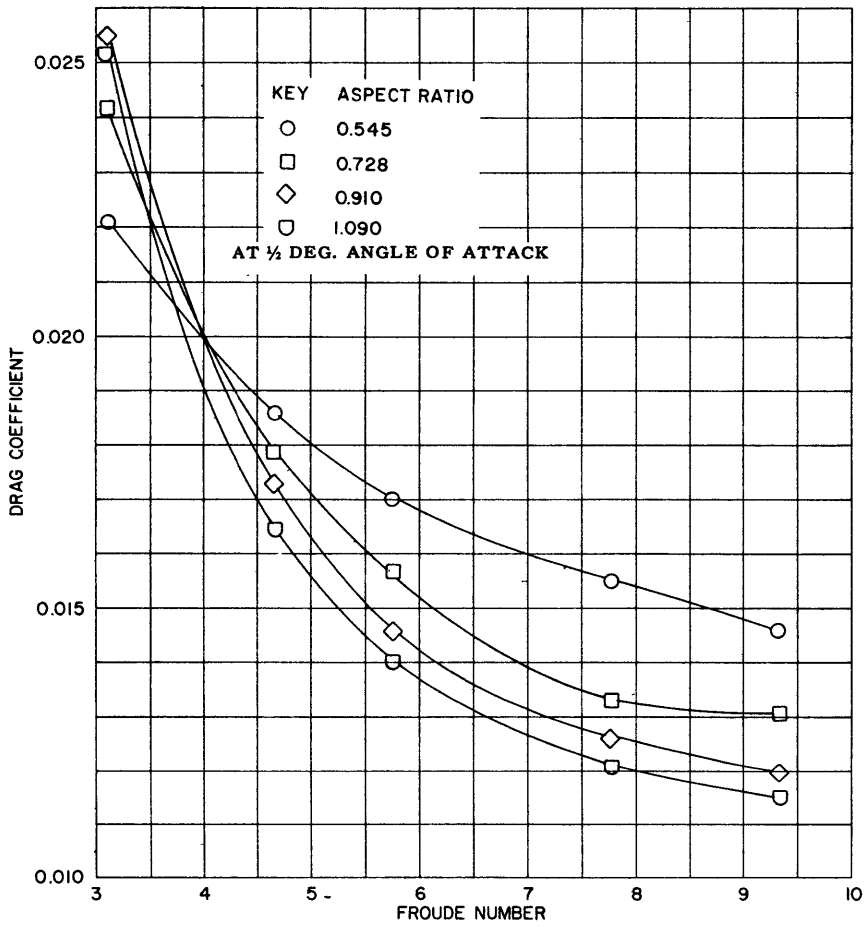

FIGURE 10- DRAG COEFFICIENT VERSUS FROUDE NUMBER FOR SECTION B

FIGURE 11 - MOMENT COEFFICIENT VERSUS ANGLE OF ATTACK FOR SECTION A

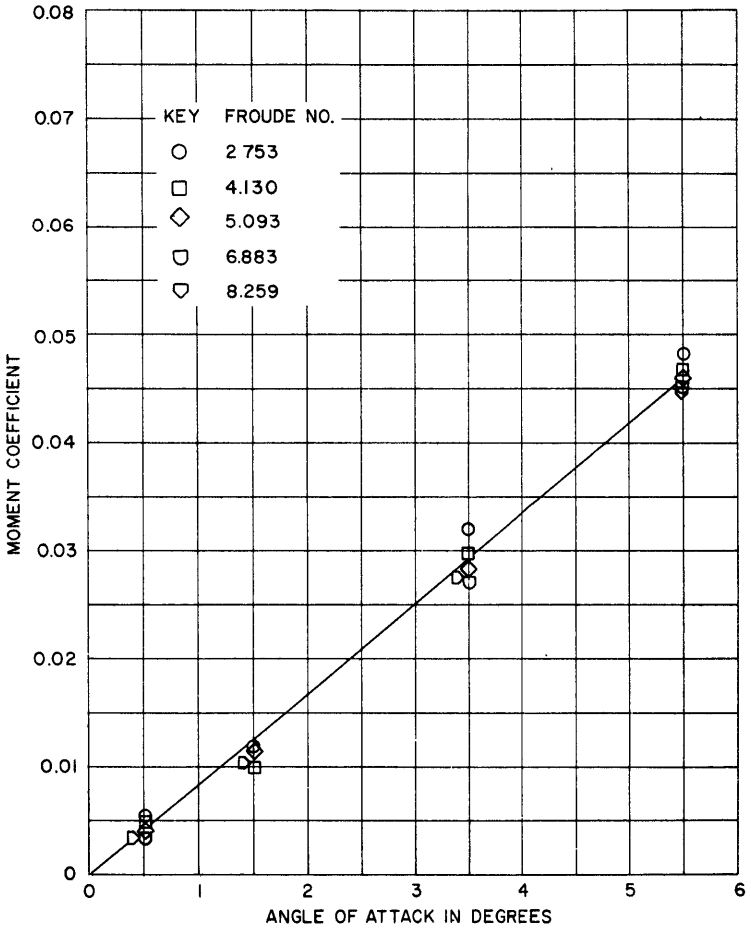

Figure 11a – Aspect Ratio = 0.429, Froude Number 2.753 to 8.259

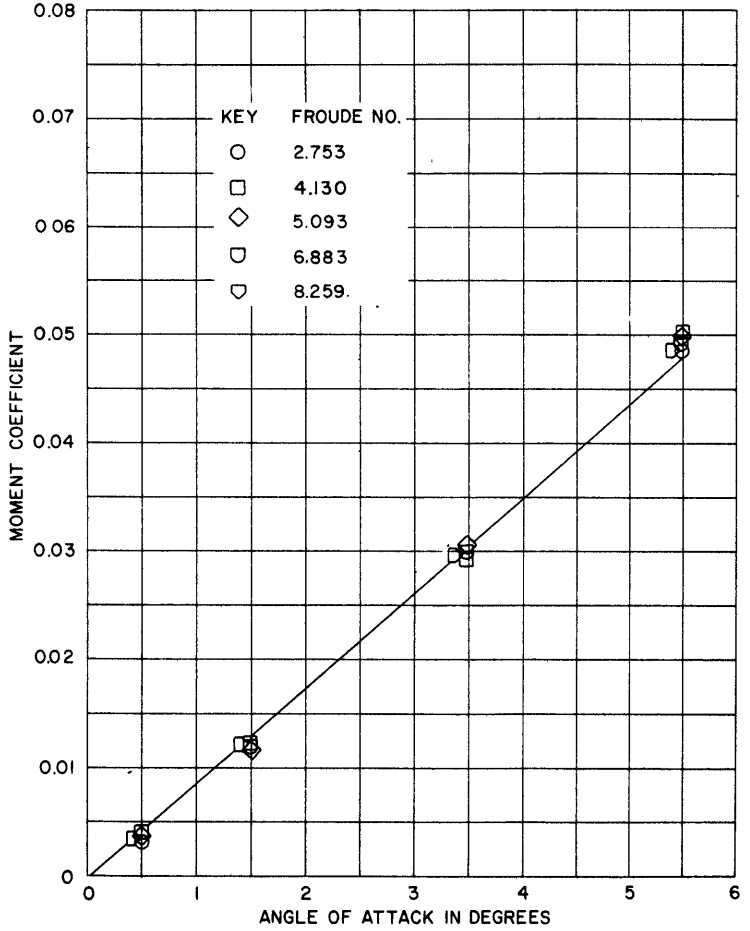

Figure 11b – Aspect Ratio = 0.571, Froude Number 2.753 to 8.259

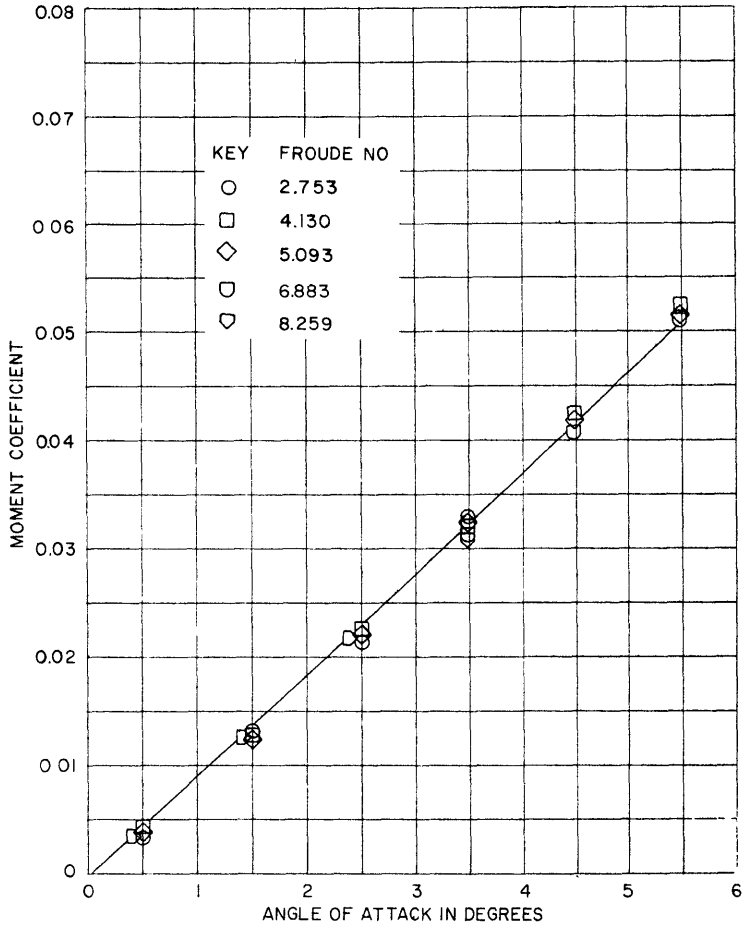

Figure 11c – Aspect Ratio = 0.715, Froude Number 2.753 to 8.259

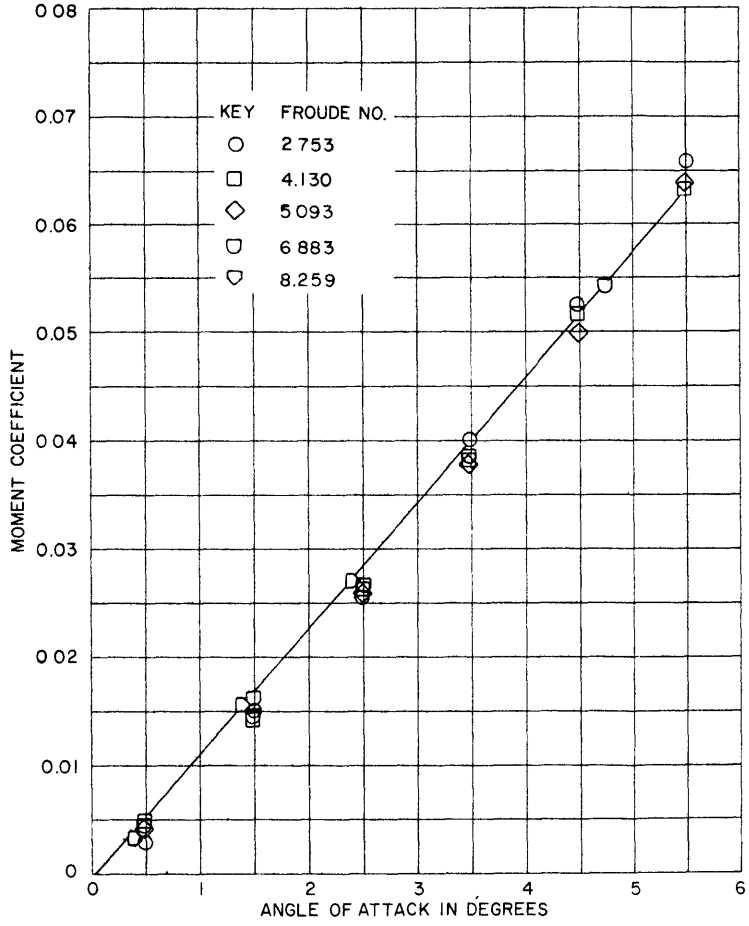

Figure 11d – Aspect Ratio = 0.858, Froude Number 2.753 to 8.259

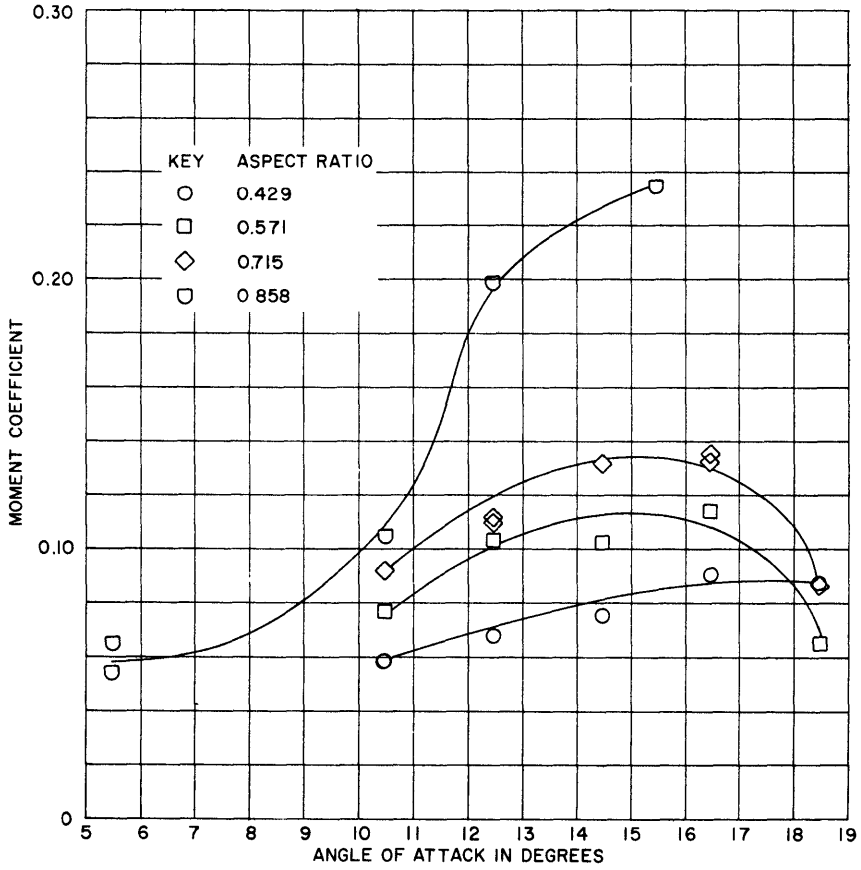

Figure 11e – Froude Number = 1.377, Aspect Ratios 0.429 to 0.858

FIGURE 12 - MOMENT COEFFICIENT VERSUS ANGLE OF ATTACK FOR SECTION B

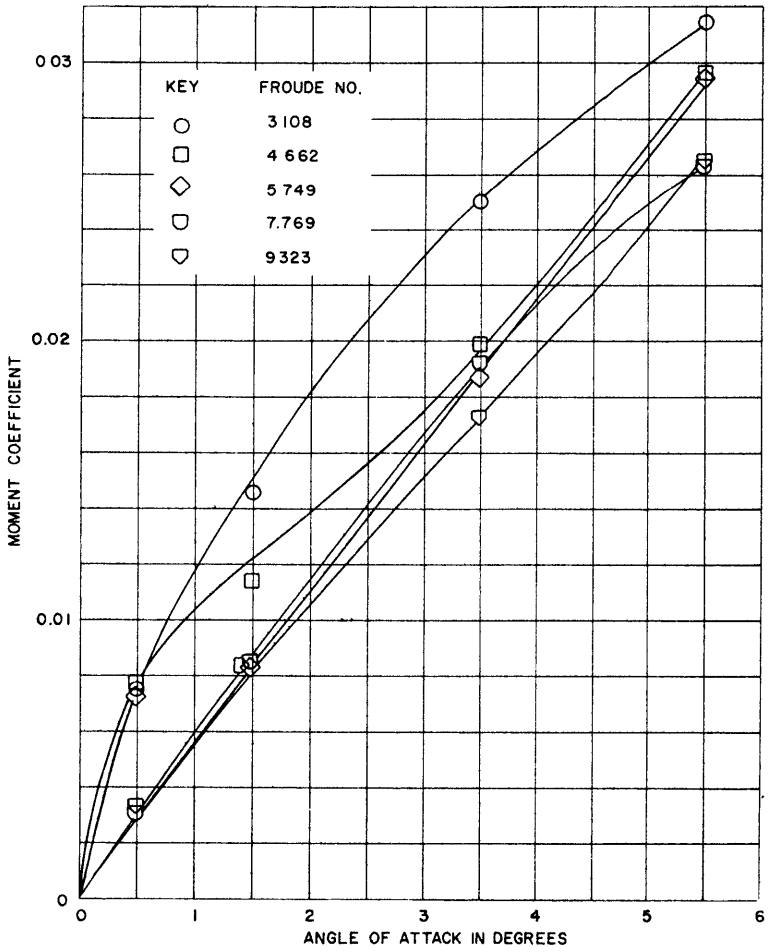

Figure 12a – Aspect Ratio = 0.545, Froude Number 3.108 to 9.323

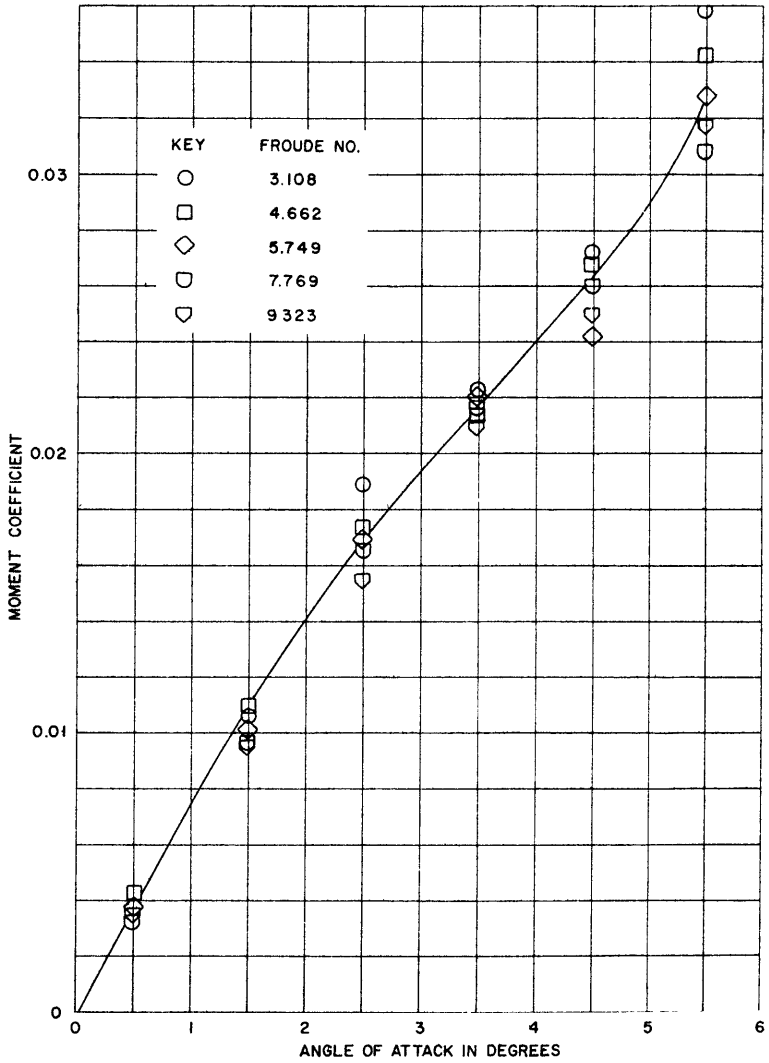

Figure 12b – Aspect Ratio = 0.728, Froude Number 3.108 to 9.323

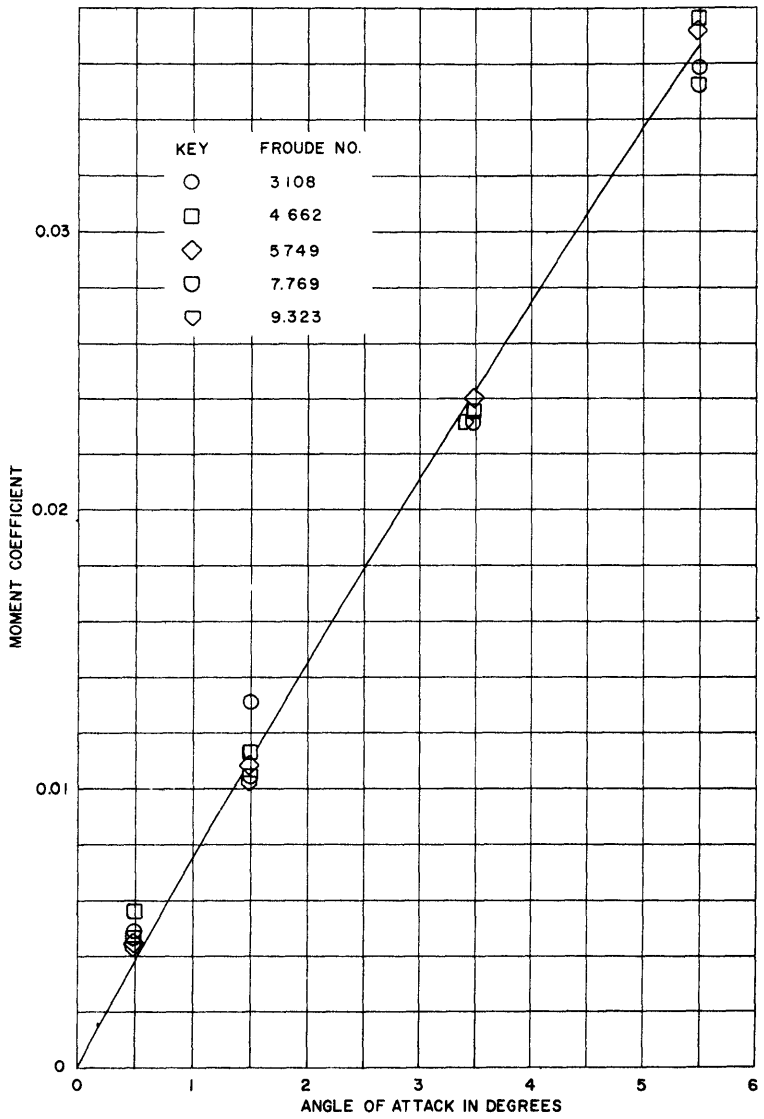

Figure 12c – Aspect Ratio = 0.910, Froude Number 3.108 to 9.323

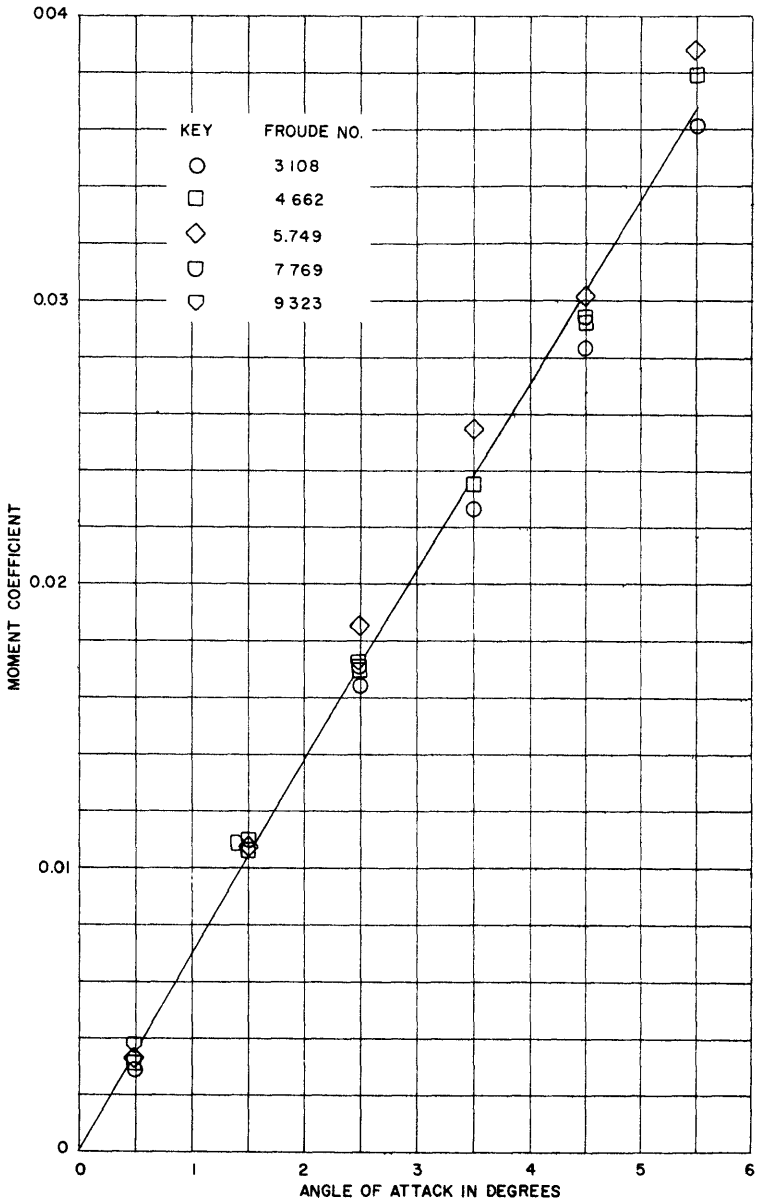

Figure 12d – Aspect Ratio = 1.090, Froude Number 3.108 to 9.323

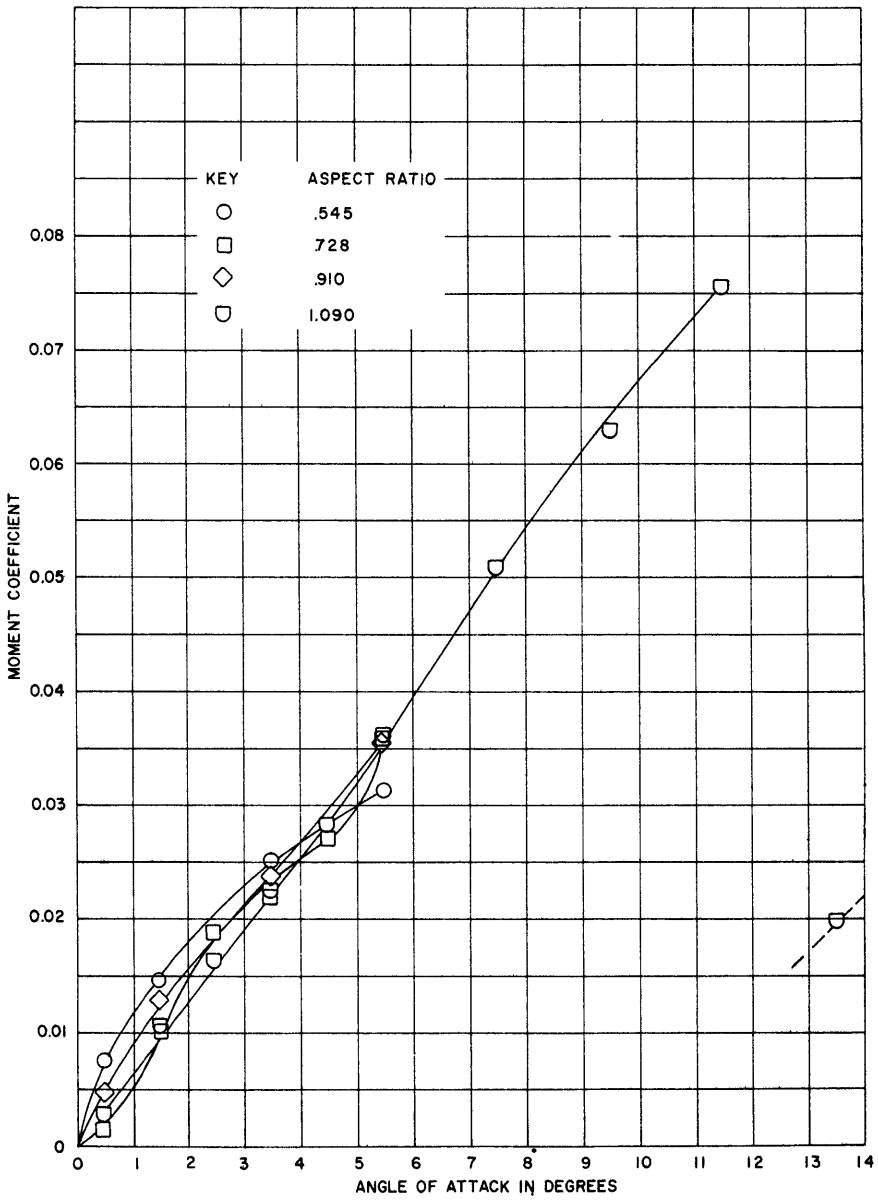

Figure 12e – Froude Number = 3.108, Aspect Ratios 0.545 to 1.090

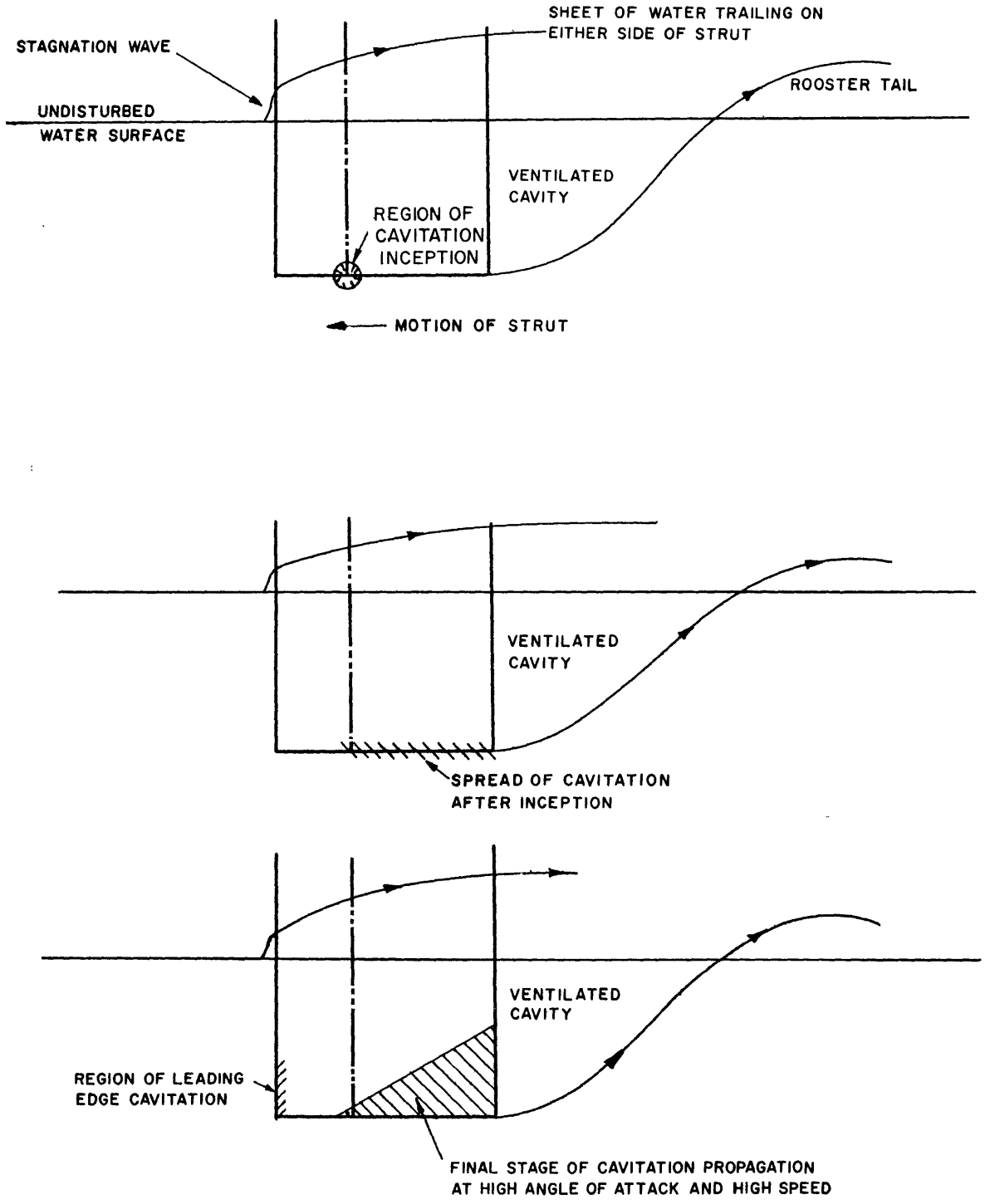

FIGURE 13 - CAVITATION DIAGRAM FOR SECTION B

SHOWING LOW PRESSURE SIDE

APPENDIX A

THEORETICAL PRESSURE DISTRIBUTIONS OF STRUT SECTIONS

In the preliminary design of the hydrofoil pitch-heave oscillator, the pressure distributions of a number of two-dimensional bodies were computed to determine a suitable (cavitation free) cross-sectional shape for the supporting struts. These pressure distributions were computed on an IBM 7090 computer by the method given in Reference 2. A total of eight shapes were considered and they are shown in Figure A1. Each shape consisted of a nose section, parallel middle body, and tail section. Two basic profiles, ogive and elliptical, were used for the nose and tail sections. The elliptical shape was chosen for its optimum cavitation properties and the ogive shape for its ease of construction. The principal dimensions and the shape designations of the eight bodies are given in Table 1, and their pressure distributions are shown in Figure A2.

TABLE I

BODY	NOSE LENGTH in.	MIDDLE BODY LENGTH in.	TAIL LENGTH in.	NOSE AND TAIL SHAPE
0-15	15	54	15	Ogive
E-15	15	54	15	Ellipse
0-20	20	48	16	Ogive
E-20	20	48	16	Ellipse
0-25	25	48	11	Ogive
E-25	25	48	11	Ellipse
0-30	30	48	6	Ogive
E-30	30	48	6	Ellipse

Middle Body Thickness = 7 in.

Total Body Length = 84 in.

Thickness: Length Ratio = 0.083

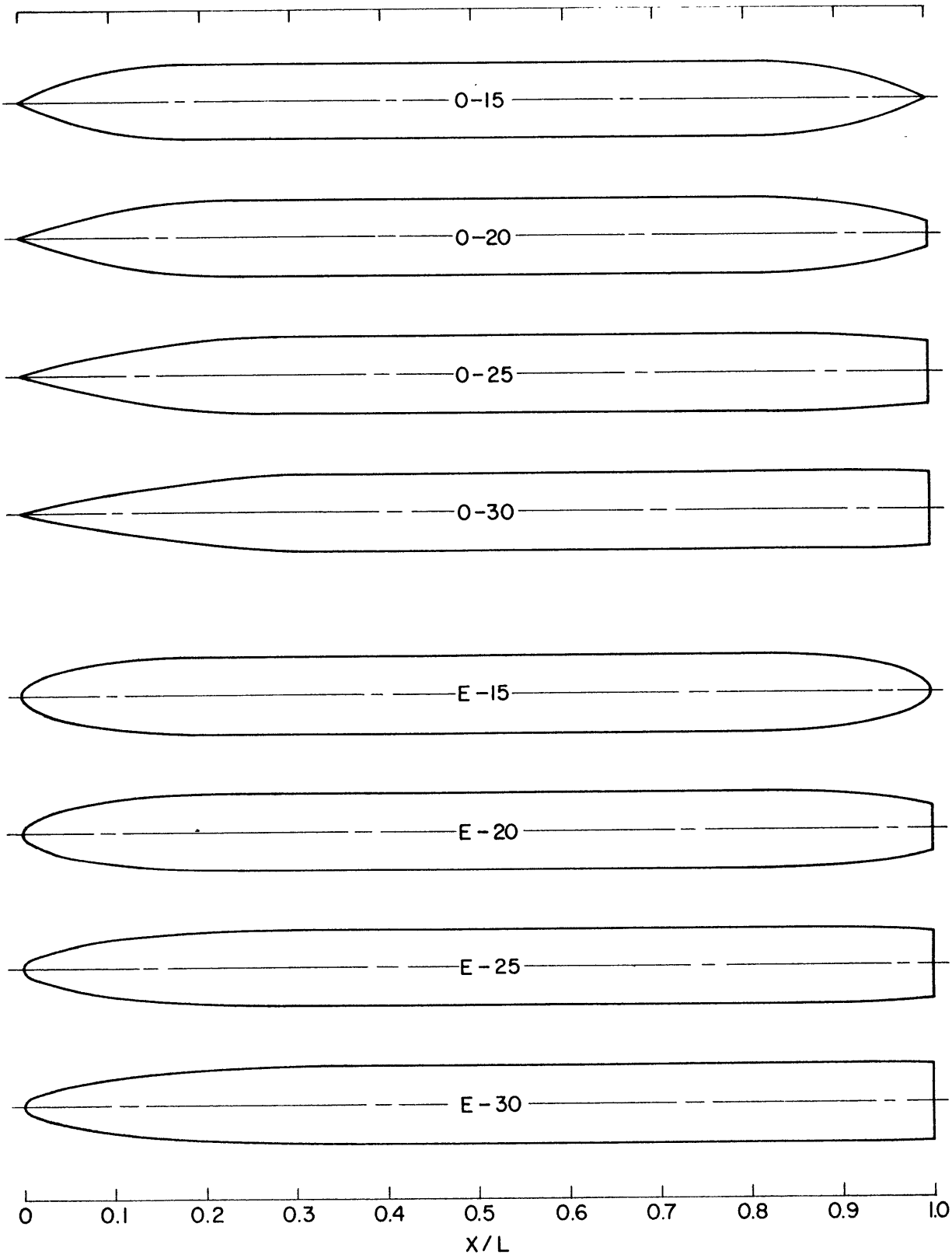

FIGURE A1 - CROSS SECTION OF STRUT BODIES STUDIED BY IBM 7090 COMPUTER

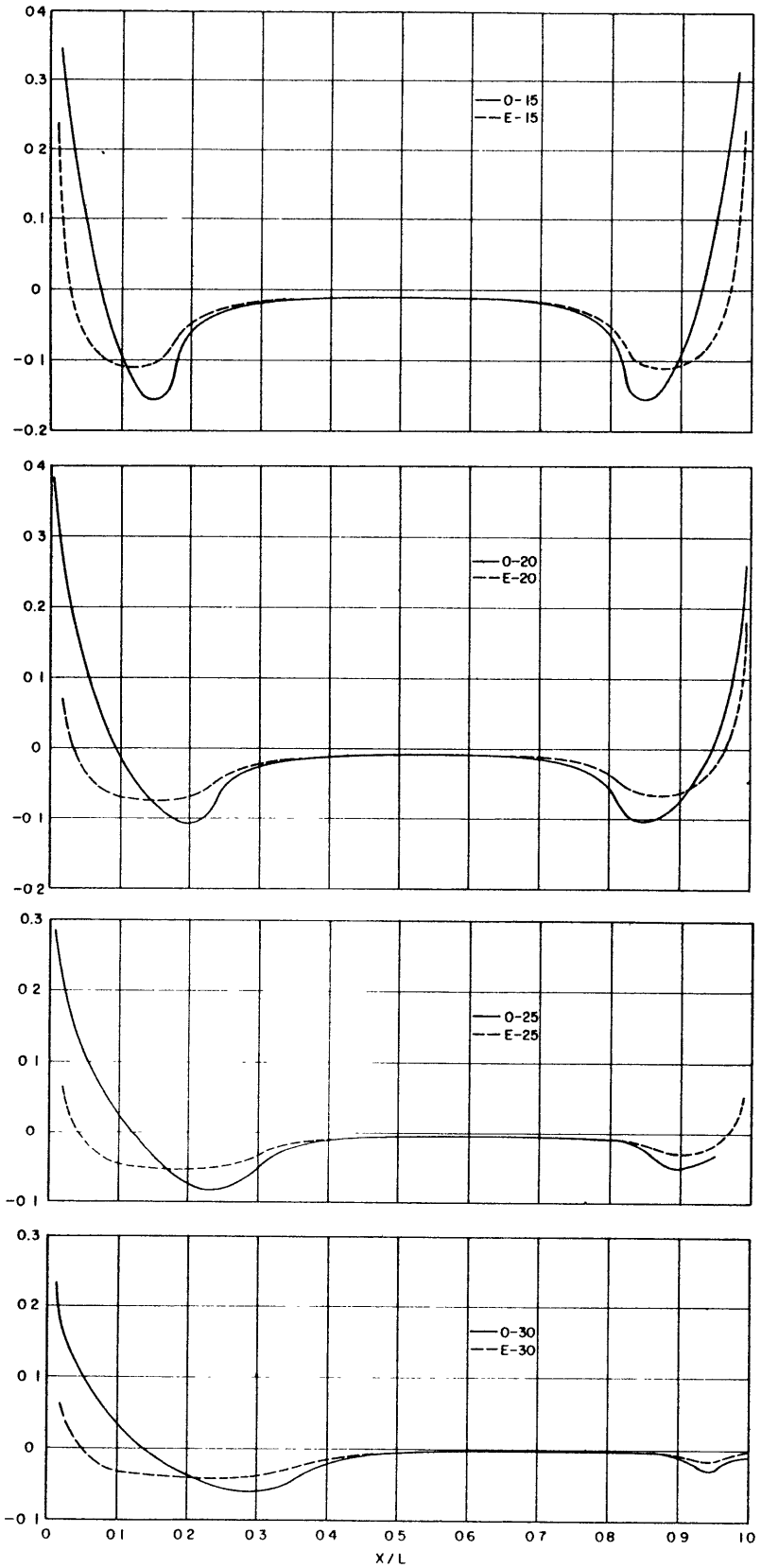

FIGURE A2 - TWO-DIMENSIONAL PRESSURE DISTRIBUTIONS ON STRUT SECTIONS

APPENDIX B

HYDRODYNAMIC LOADS ON PHO-2 STRUTS

To predict the carriage power requirements under all operating conditions, dimensional forces and moments were computed for strut B, which was selected for the PHO-2. These computations are graphically presented in Figures B1 and B2. Calculations are limited to angles of attack less than 1.5 degrees, which is the maximum angularity expected. Lift and moment were computed only for the maximum submergence. Drag was computed for four submergences.

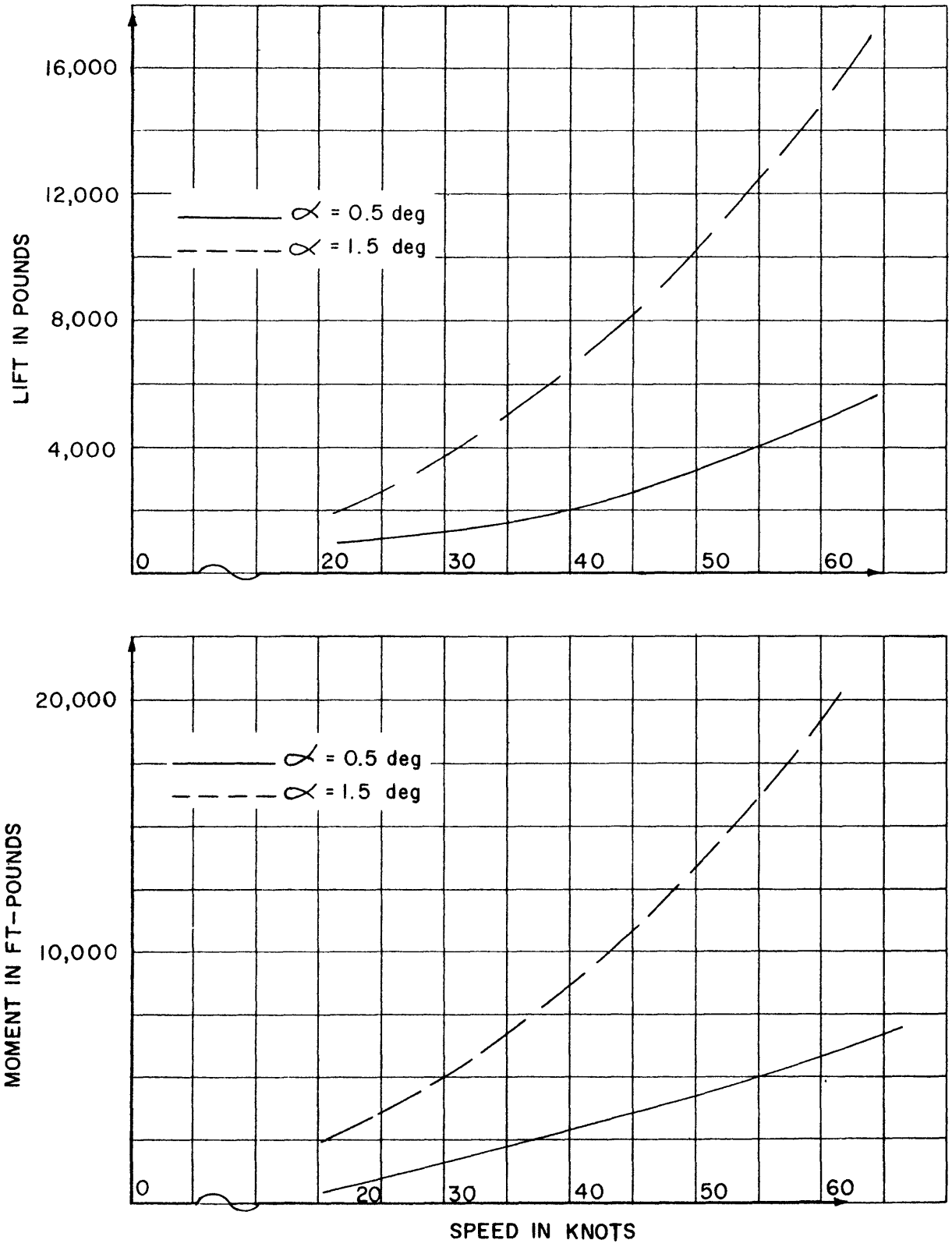

FIGURE B1 - LIFT AND MOMENT VERSUS SPEED FOR THE PHO-2 STRUT AT 6-FOOT SUBMERGENCE

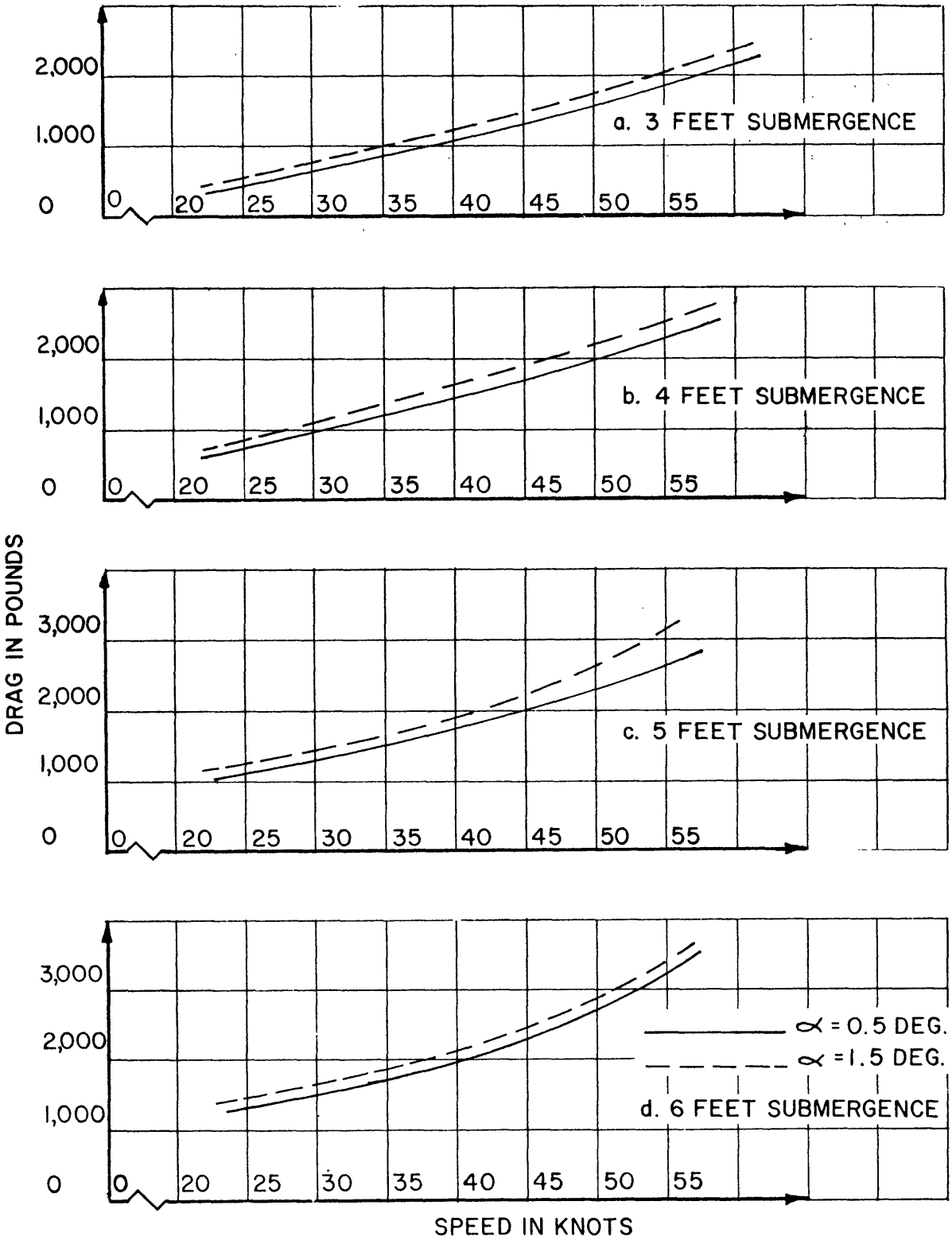

FIGURE B2 - DRAG VERSUS SPEED FOR THE PHO-2 STRUT AT VARIOUS SUBMERGENCES

REFERENCES

1. Gertler, M., "The Predicition of the Effective Horsepower of Ships by the Methods in Use at the David Taylor Model Basin," David Taylor Model Basin Report 576 (December 1957).

2. Smith, A. M. O. and Pierce, J. "Exact Solution of the Newman Problem, Calculation of Non-Circulatory Plane and Axially Symmetric Flows about or within Arbitrary Boundaries" Douglas Aircraft Company Report ES 26988 (April 1958).

INITIAL DISTRIBUTION

opies	
14	CHBUSHIPS 3 Tech Lib (Code 210L) 1 Lab Mgt (Code 320) 1 Ship Sil (Code 345) 2 Prelim Des Br (Code 420) 3 Prelim Des Sec (Code 421) 2 Hull Des Br (Code 440) 1 Sci & Res Sec (Code 442) 1 Boats & Small Craft Sec (Code 449)
20	CDR, DDC
4	CHONR 3 Fluid Dyn (Code 438) 1 Air Programs (Code 461)
1	ONR, Boston
1	ONR, New York
1	ONR, Pasadena
1	ONR, San Francisco
15	ONR, London
6	DIR, USNRL, Tech Info Div
4	CHBUWEPS 1 Code RUTO-3 1 Code RRRE 1 Code RAAD 1 Code DIS-42
1	CHBUDOCKS
1	USNOTS, China Lake
1	USNOTS, Pasadena
1	NAVSHIPYD, BSN, Planning Dept
1	NAVSHIPYD, PTSMH, Planning Dept
1	NAVSHIPYD, PEARL, Planning Dept
1	NAVSHIPYD, SFRAN, Planning Dept
1	NAVSHIPYD, MARE, Planning Dept
1	NAVSHIPYD, NYK, Planning Dept
1	NAVSHIPYD, PUG, Planning Dept

Copies	
1	NAVSHIPYD, PHILA, Planning Dept
1	NAVSHIPYD, NORVA, Planning Dept
1	NAVSHIPYD, CHASN, Planning Dept
1	NAVSHIPYD, LBEACH, Planning Dept
2	CDR, USNWEPLAB, Dahlgren 1 Planning Dept 1 Computation & Exterior Ballistic Lab Attn: Dr. A.V. Hershey
1	SUPT, USNA Attn: Lib
1	SUPT, USNAVPGSCOL
2	CMDT, USCG 1 Sec, Ship Struc Comm
2	ADMIN, MARAD 1 Div of Ship Design 1 Div of Research
1	USMMA Attn: Capt. L.S. McCready, Dept of Engineering
2	Natl BuStand, Attn: Fluid Mech Div 1 Dr. G.B. Schubauer 1 Dr. G.H. Keulegan
1	CO, Trans R & E Comm Attn: Marine Trans Div
1	DIR, NASA
1	CDR, USNOL, White Oak
2	DIR, Langley RESCEN 1 I.E. Garrick 1 Mr. D.J. Martin
1	CDR, W-PADEVCEN Attn: Mr. W. Mykytow, Dyn Br
1	Air Force Off of Sci Res Temp Bldg D. Wash 25, D.C.

Copies

1 DIR, WHOI

1 DIR, Natl Sci Foundation
Engin Sciences Div
1951 Constitution Ave, N.W.,
Wash. D.C.

3 California Inst of Tech,
Pasadena
1 Prof M.S. Plesset
1 Prof T.Y. Wu
1 Prof A.J. Acosta

3 Univ of California, Berkeley
Div of Engineering

1 Univ of California, Dept of
Engineering, Los Angeles
Attn: Dr. A. Powell

1 Dir, Scripps Inst of
Oceanography, La Jolla

1 Colorado A & M College,
Dept of Civil Engin
Fort Collins
Attn: Prof. M.L. Albertson

1 Colorado State Univ, Dept of
Civil Engin, Fort Collins
Attn: Prof J.E. Cermak

1 Cornell Univ Grad School of
Aero Engineering, Ithaca, N.Y.
Attn: Prof W.R. Sears

3 Iowa State Univ, Inst of
Hydraulic Research
Iowa City

2 Harvard Univ, Cambridge, Mass.
1 Prof G. Birkhoff, Dept of Math
1 Prof G.F. Carrier, Dept of Math

5 Massachusetts Inst of Tech,
Cambridge, Mass, Dept of NAME
1 Prof M.S. Abkowitz, Head
1 Prof A.T. Ippen
Fluid Dyn Res Lab
1 Prof H. Ashley
1 Prof M. Landahl
1 Prof J. Dugundji

4 Univ of Michigan, Ann Arbor
2 Prof R.B. Couch, Dept of Nav Arch
1 Prof W.W. Willmarth, Aero Eng Dept
1 Prof M.S. Uberoi, Aero Eng Dept

Copies

2 Dir, St Anthony Falls
Hydraulic Lab
1 Prof. B. Silberman
1 Mr. J.N. Wetzel

1 New York State Univ
Maritime College
Fort Schulter, N.Y.
Attn: Prof J.J. Foody,
Engineering Dept

3 New York University,
Inst of Math Sci
New York, N.Y.
1 Prof. J. Keller
1 Prof J.J. Stoker
1 Prof. R. Kraichuen

3 JHU, Dept of Mech Eng
Baltimore
1 Prof. S. Corrsin
2 Prof. O.M. Phillips

2 Penn State Univ,
Ord Research Lab
University Park
1 Dr. G.F. Wislicenus
1 Dr. M. Sevik

1 Rensselaer Polytechnic
Inst, Department of Math
Troy, N.Y.
Attn: Prof R.C. DiPrima

2 Davidson, SIT
1 Dr. J. Breslin
1 Mr. C.J. Henry

1 Webb Inst of Nav Arch
Glen Cove, N.Y.
Attn: Tech Lib

1 Stanford Univ, Dept of
Civil Eng
Attn: Dr. Byrne Perry

3 Univ of Md
College Park, Md.
1 Dept of Aero Eng
2 Engineering Lib

1 Hydronautics, Inc.,
Rockville, Md.
Attn: Mr. Phillip Eisenberg

Copies	
1	Rand Development Corp, Cleveland, Ohio Attn: Dr. A.S. Iberall
1	U.S. Rubber Co., Research & Development Dept, Wayne, N.J. Attn: Mr. L.M. White
1	AVCO Corp, Lycoming Div., Washington, D.C. Attn: Mr. T.A. Duncan
1	Curtiss-Wright Corp, Research Div, Turbomach Div, Quehanna, Pa. Attn: Mr. George H. Fedarson
1	Hughes Tool Co, Aircraft Div Culver City, Calif Attn: Mr. M.S. Harned
1	Lockheed Aircraft Corp, Hydrodynamics Res, Burbank, Calif Attn: Mr. Kenneth E. Hidge
1	The Rand Corp, 1700 Main St Santa Monica, Calif Attn: Mr. Blaine Parkin
1	Boeing Airplane Co., Seattle Div Seattle, Washington Attn: Mr. M.J. Turner
2	Cornell Aeronautical Lab, 4455 Genesee St, Buffalo, N.Y. Attn: Dr. I. Statler Mr. R. White
1	Electric Boat Div, Gen Dyn Corp Groton, Conn Attn: Mr. R. McCandliss
1	Gibbs & Cox, Inc., 21 West St New York, N.Y.
1	General Applied Sci Labs, Inc Merrick & Stewart Avenues, Westbury, L.I., N.Y. Attn: Dr. F. Lane
2	Grumman Aircraft Eng Corp Bethpage, L.I., N.Y. Attn: Mr. E. Baird Mr. C. Squires

Copies	
1	Lockheed Aircraft Corp, Missiles & Space Div. Palo Alto, Calif Attn: Mr. R.W. Kermeen
1	Midwest Research Inst, 425 Volker Blvd Kansas City 10, Mo. Attn: Mr. Zydel
3	Southwest Research Inst, Dept of Mech Sciences 8500 Culebra Rd., San Antonia 6, Texas Attn: Dr. H.N. Abramson Mr. G. Ransleben Editor, Applied Mech Review
1	Oceanics Inc., 114 East 40th St New York 16, N.Y. Attn: Dr. P. Kaplan
2	Consolidated Systems Corp. 600 East Bonita Ave Pomona, Calif Attn: Mr. Arthur A. Burgess

Unclassified

Security Classification

DOCUMENT CONTROL DATA - R&D

(Security classification of title, body of abstract and indexing annotation must be entered when the overall report is classified)

1 ORIGINATING ACTIVITY (Corporate author)	2a. REPORT SECURITY CLASSIFICATION
David Taylor Model Basin	Unclassified
	2b GROUP

3 REPORT TITLE

EXPERIMENTAL MEASUREMENTS OF THE STEADY LIFT, DRAG, AND MOMENT ON SURFACE-PIERCING STRUTS

4. DESCRIPTIVE NOTES (Type of report and inclusive dates)

Final

5. AUTHOR(S) (Last name, first name, initial)

Wilburn, Gene M. and Haller, H. Smith

6. REPORT DATE	7a TOTAL NO OF PAGES	7b. NO OF REFS
October 1965	49	2

8a CONTRACT OR GRANT NO.	9a ORIGINATOR'S REPORT NUMBER(S)
b. PROJECT NO. SS 600,000	1778
c. Task 1703	9b. OTHER REPORT NO(S) (Any other numbers that may be assigned this report)
d	

10 AVAILABILITY/LIMITATION NOTICES

Qualified requesters may obtain copies of this report from DDC

11 SUPPLEMENTARY NOTES	12. SPONSORING MILITARY ACTIVITY
	Bureau of Ships

13 ABSTRACT

Testing of two surface-piercing strut configurations for the TMB Pitch-Heave Oscillator is described. Experimental measurements were made of the steady lift, drag, and moment on two rectangular planform, finite aspect ratio struts at finite Froude numbers. The first model section had idential symmetrical ogival fairings on the leading and trailing edges and a flat center section. For the second configuration the aft ogive fairing was cut off the first model section, and a square trailing edge was left. The model force and moment coefficients are presented and the wake, spray, and cavitation characteristics of both profiles are discussed.

Preliminary computations of the theoretical pressure distributions for 8 two-dimensional sections and computed full-scale forces and moments for the PHO-2 strut configuration are included.

DD FORM 1 JAN 64 1473

Unclassified

Security Classification

14. KEY WORDS	LINK A		LINK B		LINK C	
	ROLE	WT	ROLE	WT	ROLE	WT
Surface piercing struts Ogive fairing Blunt trailing edge Aspect ratio Wake Spray Lift and Drag coefficients Moment coefficient Pressure distribution Cavitation Angle of attack						

INSTRUCTIONS

1. ORIGINATING ACTIVITY: Enter the name and address of the contractor, subcontractor, grantee, Department of Defense activity or other organization *(corporate author)* issuing the report.

2*a*. REPORT SECURITY CLASSIFICATION: Enter the overall security classification of the report. Indicate whether "Restricted Data" is included. Marking is to be in accordance with appropriate security regulations.

2*b*. GROUP: Automatic downgrading is specified in DoD Directive 5200.10 and Armed Forces Industrial Manual. Enter the group number. Also, when applicable, show that optional markings have been used for Group 3 and Group 4 as authorized.

3. REPORT TITLE: Enter the complete report title in all capital letters. Titles in all cases should be unclassified. If a meaningful title cannot be selected without classification, show title classification in all capitals in parenthesis immediately following the title.

4. DESCRIPTIVE NOTES: If appropriate, enter the type of report, e.g., interim, progress, summary, annual, or final. Give the inclusive dates when a specific reporting period is covered.

5. AUTHOR(S): Enter the name(s) of author(s) as shown on or in the report. Enter last name, first name, middle initial. If military, show rank and branch of service. The name of the principal author is an absolute minimum requirement.

6. REPORT DATE: Enter the date of the report as day, month, year; or month, year. If more than one date appears on the report, use date of publication.

7*a*. TOTAL NUMBER OF PAGES: The total page count should follow normal pagination procedures, i.e., enter the number of pages containing information.

7*b*. NUMBER OF REFERENCES: Enter the total number of references cited in the report.

8*a*. CONTRACT OR GRANT NUMBER: If appropriate, enter the applicable number of the contract or grant under which the report was written.

8*b*, 8*c*, & 8*d*. PROJECT NUMBER: Enter the appropriate military department identification, such as project number, subproject number, system numbers, task number, etc.

9*a*. ORIGINATOR'S REPORT NUMBER(S): Enter the official report number by which the document will be identified and controlled by the originating activity. This number must be unique to this report.

9*b*. OTHER REPORT NUMBER(S): If the report has been assigned any other report numbers *(either by the originator or by the sponsor)*, also enter this number(s).

10. AVAILABILITY/LIMITATION NOTICES: Enter any limitations on further dissemination of the report, other than those imposed by security classification, using standard statements such as:

(1) "Qualified requesters may obtain copies of this report from DDC."

(2) "Foreign announcement and dissemination of this report by DDC is not authorized."

(3) "U. S. Government agencies may obtain copies of this report directly from DDC. Other qualified DDC users shall request through _____."

(4) "U. S. military agencies may obtain copies of this report directly from DDC. Other qualified users shall request through _____."

(5) "All distribution of this report is controlled. Qualified DDC users shall request through _____."

If the report has been furnished to the Office of Technical Services, Department of Commerce, for sale to the public, indicate this fact and enter the price, if known.

11. SUPPLEMENTARY NOTES: Use for additional explanatory notes.

12. SPONSORING MILITARY ACTIVITY: Enter the name of the departmental project office or laboratory sponsoring *(paying for)* the research and development. Include address.

13. ABSTRACT: Enter an abstract giving a brief and factual summary of the document indicative of the report, even though it may also appear elsewhere in the body of the technical report. If additional space is required, a continuation sheet shall be attached.

It is highly desirable that the abstract of classified reports be unclassified. Each paragraph of the abstract shall end with an indication of the military security classification of the information in the paragraph, represented as *(TS), (S), (C), or (U)*

There is no limitation on the length of the abstract. However, the suggested length is from 150 to 225 words.

14. KEY WORDS: Key words are technically meaningful terms or short phrases that characterize a report and may be used as index entries for cataloging the report. Key words must be selected so that no security classification is required. Identifiers, such as equipment model designation, trade name, military project code name, geographic location, may be used as key words but will be followed by an indication of technical context. The assignment of links, roles, and weights is optional.

David Taylor Model Basin. Report 1778.
EXPERIMENTAL MEASUREMENTS OF THE STEADY LIFT, DRAG, AND MOMENT ON SURFACE PIERCING STRUTS, by Gene M. Wilburn and H. Smith Haller, Jr., Oct 1965. iv, 49p., illus., diags., graphs, refs. UNCLASSIFIED

Testing of two surface-piercing strut configurations for the TMB Pitch-Heave Oscillator is described. Experimental measurements were made of the steady lift, drag, and moment on two rectangular planform, finite aspect ratio struts at finite Froude numbers. The first model section had identical symmetrical ogival fairings on the leading and trailing edges and a flat center section. For the second configuration the aft ogive fairing was cut off the first model section, and a square trailing edge was

1. Struts--Lift--Measurements
2. Struts--Drag--Measurements
3. Struts--Wake--Measurement
4. Struts--Cavitation--Measurement
5. Angle of Attack--Forces--Measurement
6. Dynamometers--TMB 3-component

I. Wilburn, Gene M.
II. Haller, H. Smith

David Taylor Model Basin. Report 1778.
EXPERIMENTAL MEASUREMENTS OF THE STEADY LIFT, DRAG, AND MOMENT ON SURFACE PIERCING STRUTS, by Gene M. Wilburn and H. Smith Haller, Jr., Oct 1965. iv, 49p., illus., diags., graphs, refs. UNCLASSIFIED

Testing of two surface-piercing strut configurations for the TMB Pitch-Heave Oscillator is described. Experimental measurements were made of the steady lift, drag, and moment on two rectangular planform, finite aspect ratio struts at finite Froude numbers. The first model section had identical symmetrical ogival fairings on the leading and trailing edges and a flat center section. For the second configuration the aft ogive fairing was cut off the first model section, and a square trailing edge was

1. Struts--Lift--Measurements
2. Struts--Drag--Measurements
3. Struts--Wake--Measurement
4. Struts--Cavitation--Measurement
5. Angle of Attack--Forces--Measurement
6. Dynamometers--TMB 3-component

I. Wilburn, Gene M.
II. Haller, H. Smith

David Taylor Model Basin. Report 1778.
EXPERIMENTAL MEASUREMENTS OF THE STEADY LIFT, DRAG, AND MOMENT ON SURFACE PIERCING STRUTS, by Gene M. Wilburn and H. Smith Haller, Jr., Oct 1965. iv, 49p., illus., diags., graphs, refs. UNCLASSIFIED

Testing of two surface-piercing strut configurations for the TMB Pitch-Heave Oscillator is described. Experimental measurements were made of the steady lift, drag, and moment on two rectangular planform, finite aspect ratio struts at finite Froude numbers. The first model section had identical symmetrical ogival fairings on the leading and trailing edges and a flat center section. For the second configuration the aft ogive fairing was cut off the first model section, and a square trailing edge was

1. Struts--Lift--Measurements
2. Struts--Drag--Measurements
3. Struts--Wake--Measurement
4. Struts--Cavitation--Measurement
5. Angle of Attack--Forces--Measurement
6. Dynamometers--TMB 3-component

I. Wilburn, Gene M.
II. Haller, H. Smith

David Taylor Model Basin. Report 1778.
EXPERIMENTAL MEASUREMENTS OF THE STEADY LIFT, DRAG, AND MOMENT ON SURFACE PIERCING STRUTS, by Gene M. Wilburn and H. Smith Haller, Jr., Oct 1965. iv, 49p., illus., diags., graphs, refs. UNCLASSIFIED

Testing of two surface-piercing strut configurations for the TMB Pitch-Heave Oscillator is described. Experimental measurements were made of the steady lift, drag, and moment on two rectangular planform, finite aspect ratio struts at finite Froude numbers. The first model section had identical symmetrical ogival fairings on the leading and trailing edges and a flat center section. For the second configuration the aft ogive fairing was cut off the first model section, and a square trailing edge was

1. Struts--Lift--Measurements
2. Struts--Drag--Measurements
3. Struts--Wake--Measurement
4. Struts--Cavitation--Measurement
5. Angle of Attack--Forces--Measurement
6. Dynamometers--TMB 3-component

I. Wilburn, Gene M.
II. Haller, H. Smith

left. The model force and moment coefficients are presented and the wake, spray, and cavitation characteristics of both profiles are discussed.

Preliminary computations of the theoretical pressure distributions for 8 two-dimensional sections and computed full-scale forces and moments for the PHO-2 strut configuration are included.

left. The model force and moment coefficients are presented and the wake, spray, and cavitation characteristics of both profiles are discussed.

Preliminary computations of the theoretical pressure distributions for 8 two-dimensional sections and computed full-scale forces and moments for the PHO-2 strut configuration are included.

left. The model force and moment coefficients are presented and the wake, spray, and cavitation characteristics of both profiles are discussed.

Preliminary computations of the theoretical pressure distributions for 8 two-dimensional sections and computed full-scale forces and moments for the PHO-2 strut configuration are included.

left. The model force and moment coefficients are presented and the wake, spray, and cavitation characteristics of both profiles are discussed.

Preliminary computations of the theoretical pressure distributions for 8 two-dimensional sections and computed full-scale forces and moments for the PHO-2 strut configuration are included.

David Taylor Model Basin. Report 1778.
EXPERIMENTAL MEASUREMENTS OF THE STEADY LIFT, DRAG, AND MOMENT ON SURFACE PIERCING STRUTS, by Gene M. Wilburn and H. Smith Haller, Jr., Oct 1965. iv, 49p., illus., diags., graphs, refs. UNCLASSIFIED

Testing of two surface-piercing strut configurations for the TMB Pitch-Heave Oscillator is described. Experimental measurements were made of the steady lift, drag, and moment on two rectangular planform, finite aspect ratio struts at finite Froude numbers. The first model section had identical symmetrical ogival fairings on the leading and trailing edges and a flat center section. For the second configuration the aft ogive fairing was cut off the first model section, and a square trailing edge was

1. Struts--Lift--Measurements
2. Struts--Drag--Measurements
3. Struts--Wake--Measurement
4. Struts--Cavitation--Measurement
5. Angle of Attack--Forces--Measurement
6. Dynamometers--TMB 3-component
I. Wilburn, Gene M.
II. Haller, H. Smith

David Taylor Model Basin. Report 1778.
EXPERIMENTAL MEASUREMENTS OF THE STEADY LIFT, DRAG, AND MOMENT ON SURFACE PIERCING STRUTS, by Gene M. Wilburn and H. Smith Haller, Jr., Oct 1965. iv, 49p., illus., diags., graphs, refs. UNCLASSIFIED

Testing of two surface-piercing strut configurations for the TMB Pitch-Heave Oscillator is described. Experimental measurements were made of the steady lift, drag, and moment on two rectangular planform, finite aspect ratio struts at finite Froude numbers. The first model section had identical symmetrical ogival fairings on the leading and trailing edges and a flat center section. For the second configuration the aft ogive fairing was cut off the first model section, and a square trailing edge was

1. Struts--Lift--Measurements
2. Struts--Drag--Measurements
3. Struts--Wake--Measurement
4. Struts--Cavitation--Measurement
5. Angle of Attack--Forces--Measurement
6. Dynamometers--TMB 3-component
I. Wilburn, Gene M.
II. Haller, H. Smith

David Taylor Model Basin. Report 1778.
EXPERIMENTAL MEASUREMENTS OF THE STEADY LIFT, DRAG, AND MOMENT ON SURFACE PIERCING STRUTS, by Gene M. Wilburn and H. Smith Haller, Jr., Oct 1965. iv, 49p., illus., diags., graphs, refs. UNCLASSIFIED

Testing of two surface-piercing strut configurations for the TMB Pitch-Heave Oscillator is described. Experimental measurements were made of the steady lift, drag, and moment on two rectangular planform, finite aspect ratio struts at finite Froude numbers. The first model section had identical symmetrical ogival fairings on the leading and trailing edges and a flat center section. For the second configuration the aft ogive fairing was cut off the first model section, and a square trailing edge was

1. Struts--Lift--Measurements
2. Struts--Drag--Measurements
3. Struts--Wake--Measurement
4. Struts--Cavitation--Measurement
5. Angle of Attack--Forces--Measurement
6. Dynamometers--TMB 3-component
I. Wilburn, Gene M.
II. Haller, H. Smith

David Taylor Model Basin. Report 1778.
EXPERIMENTAL MEASUREMENTS OF THE STEADY LIFT, DRAG, AND MOMENT ON SURFACE PIERCING STRUTS, by Gene M. Wilburn and H. Smith Haller, Jr., Oct 1965. iv, 49p., illus., diags., graphs, refs. UNCLASSIFIED

Testing of two surface-piercing strut configurations for the TMB Pitch-Heave Oscillator is described. Experimental measurements were made of the steady lift, drag, and moment on two rectangular planform, finite aspect ratio struts at finite Froude numbers. The first model section had identical symmetrical ogival fairings on the leading and trailing edges and a flat center section. For the second configuration the aft ogive fairing was cut off the first model section, and a square trailing edge was

1. Struts--Lift--Measurements
2. Struts--Drag--Measurements
3. Struts--Wake--Measurement
4. Struts--Cavitation--Measurement
5. Angle of Attack--Forces--Measurement
6. Dynamometers--TMB 3-component
I. Wilburn, Gene M.
II. Haller, H. Smith

left. The model force and moment coefficients are presented and the wake, spray, and cavitation characteristics of both profiles are discussed.

Preliminary computations of the theoretical pressure distributions for 8 two-dimensional sections and computed full-scale forces and moments for the PHO-2 strut configuration are included.

left. The model force and moment coefficients are presented and the wake, spray, and cavitation characteristics of both profiles are discussed.

Preliminary computations of the theoretical pressure distributions for 8 two-dimensional sections and computed full-scale forces and moments for the PHO-2 strut configuration are included.

left. The model force and moment coefficients are presented and the wake, spray, and cavitation characteristics of both profiles are discussed.

Preliminary computations of the theoretical pressure distributions for 8 two-dimensional sections and computed full-scale forces and moments for the PHO-2 strut configuration are included.

left. The model force and moment coefficients are presented and the wake, spray, and cavitation characteristics of both profiles are discussed.

Preliminary computations of the theoretical pressure distributions for 8 two-dimensional sections and computed full-scale forces and moments for the PHO-2 strut configuration are included.